Nucleon EM Form Factors in BESIII

Samer Ahmed[1,2], Alaa Dbeyssi[1], Paul Larin[2], Dexu Lin[1,2], Frank Maas[1,2,3],
Cristina Morales[1], Christoph Rosner[1,2], Yadi Wang[1]
and BESIII Collaboration

1.Helmholtz-Institut Mainz, 55128 Mainz, Germany
2.Institut für Kernphysik, JGU Mainz, 55099 Mainz, Germany
3.PRISMA Cluster of Excellence, JGU Mainz, 55099 Mainz, Germany

ECT* Workshop 'Probing transverse nucleon structure at high momentum transfer'
18th – 22nd April 2016, Trento (Italia)

Outline

- BESIII@BEPCII
- Motivation
- Proton TL EM form factors in BESIII
- Neutron TL EM form factors in BESIII
- Summary

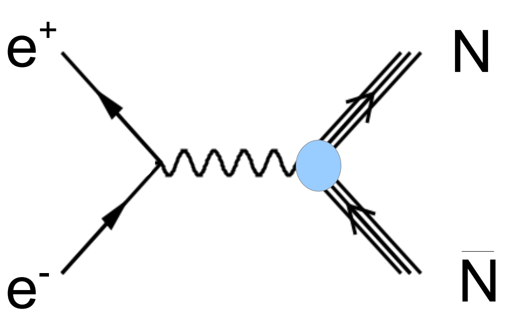

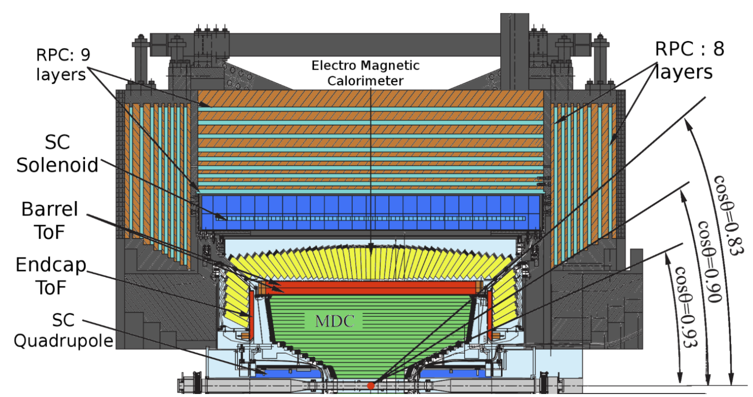

Completely new detector
Comparable performance to CLEO-c, + muon ID

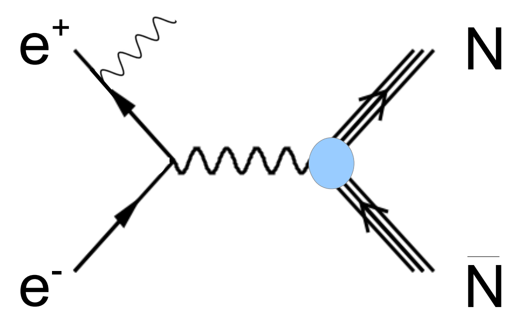

BESIII@BEPCII

BEPCII Collider

Symmetric e^+e^--collider (double rings)
Beam Energy: 1.0 – 2.3 GeV
Crossing angle: 11mrad
Design Luminosity 10^{33} cm^{-2} s^{-1}
Energy spread: $5.16 \cdot 10^{-4}$

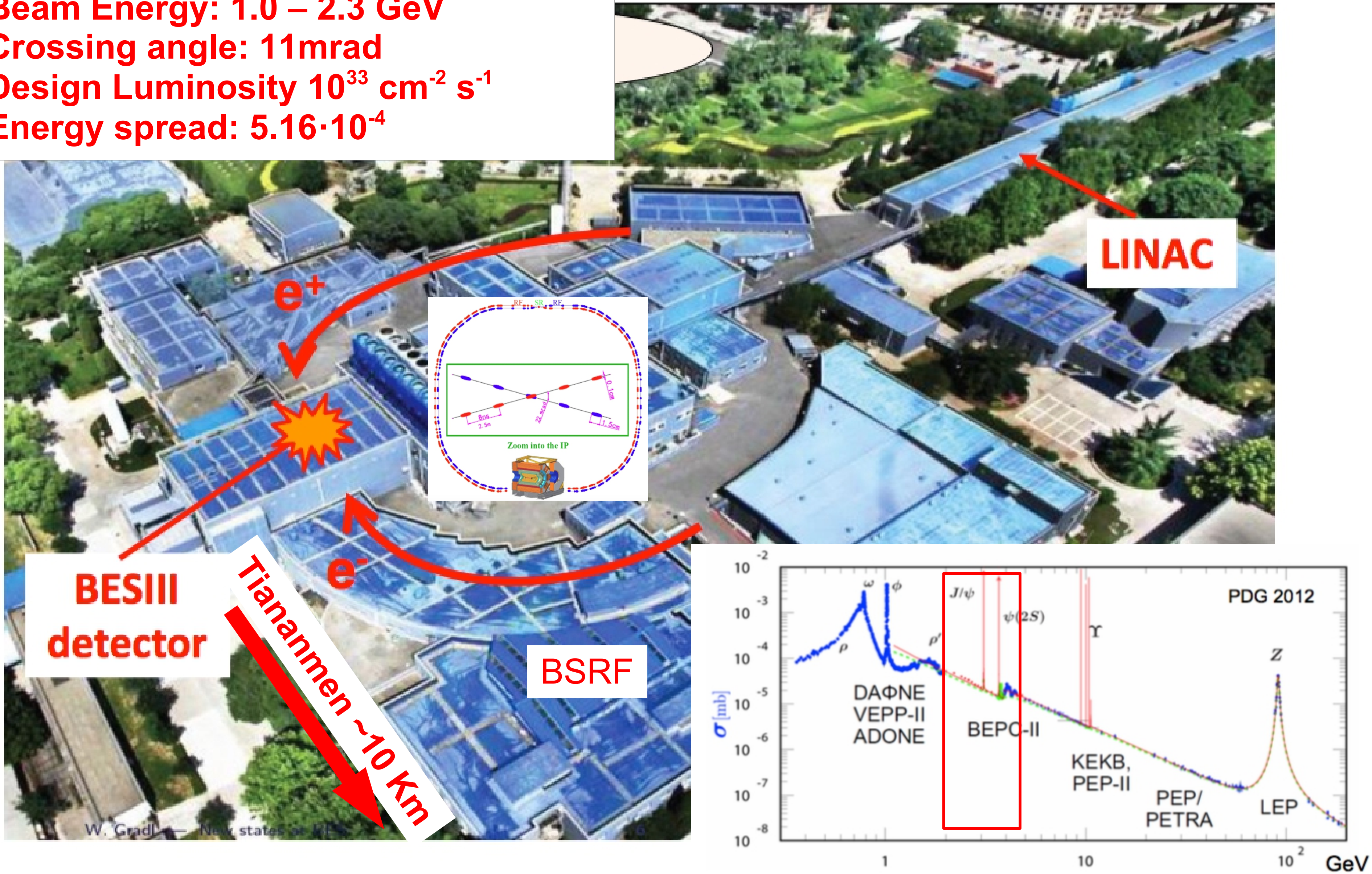

BESIII Detector

[Nucl. Instr. Meth. A614, 345 (2010)]

MDC

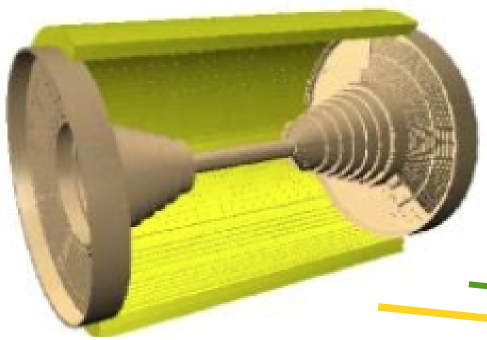

R inner: 63mm
R outer: 810 mm
Length: 2582 mm
43 Layers

$\sigma(p)/p < 0.5\%$
$\sigma_{dE/dx}/dE/dx < 6\%$

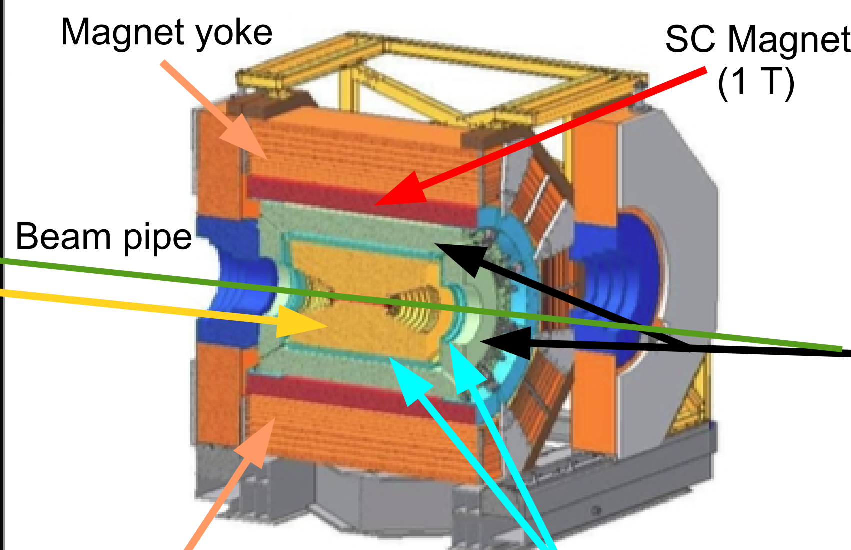

CsI(Tl) EMC

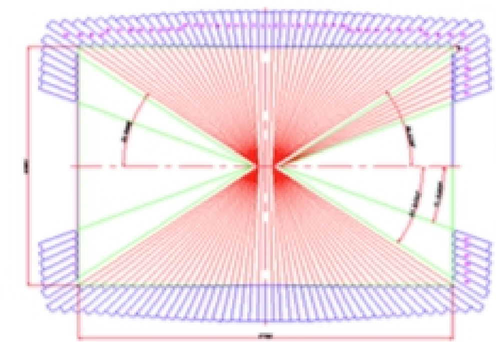

6240 CsI(Tl) crystals: 28cm (**15X_0**)
Barrel: $|\cos\Theta|<0.83$
Endcap: $0.85 < |\cos\Theta| < 0.93$

$\sigma(E)/E < 2.5\%$
$\sigma_{Z,\Phi}(E) = 0.5 - 0.7$ cm

RPC MUC

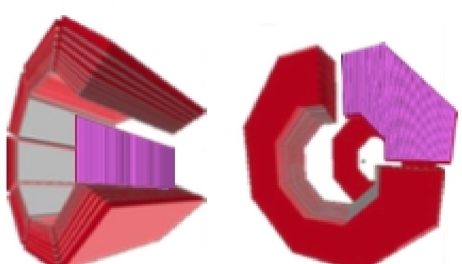

8 – 9 layers of RPC
p>400 MeV/c
$\delta R\Phi = 1.4 \sim 1.7$ cm

TOF

BTOF: two layers;
ETOF: 48 crys. for each

$\sigma(t) = 80ps$ (barrel)
$\sigma(t) = 120ps$ (endcap)

BESIII Data Samples

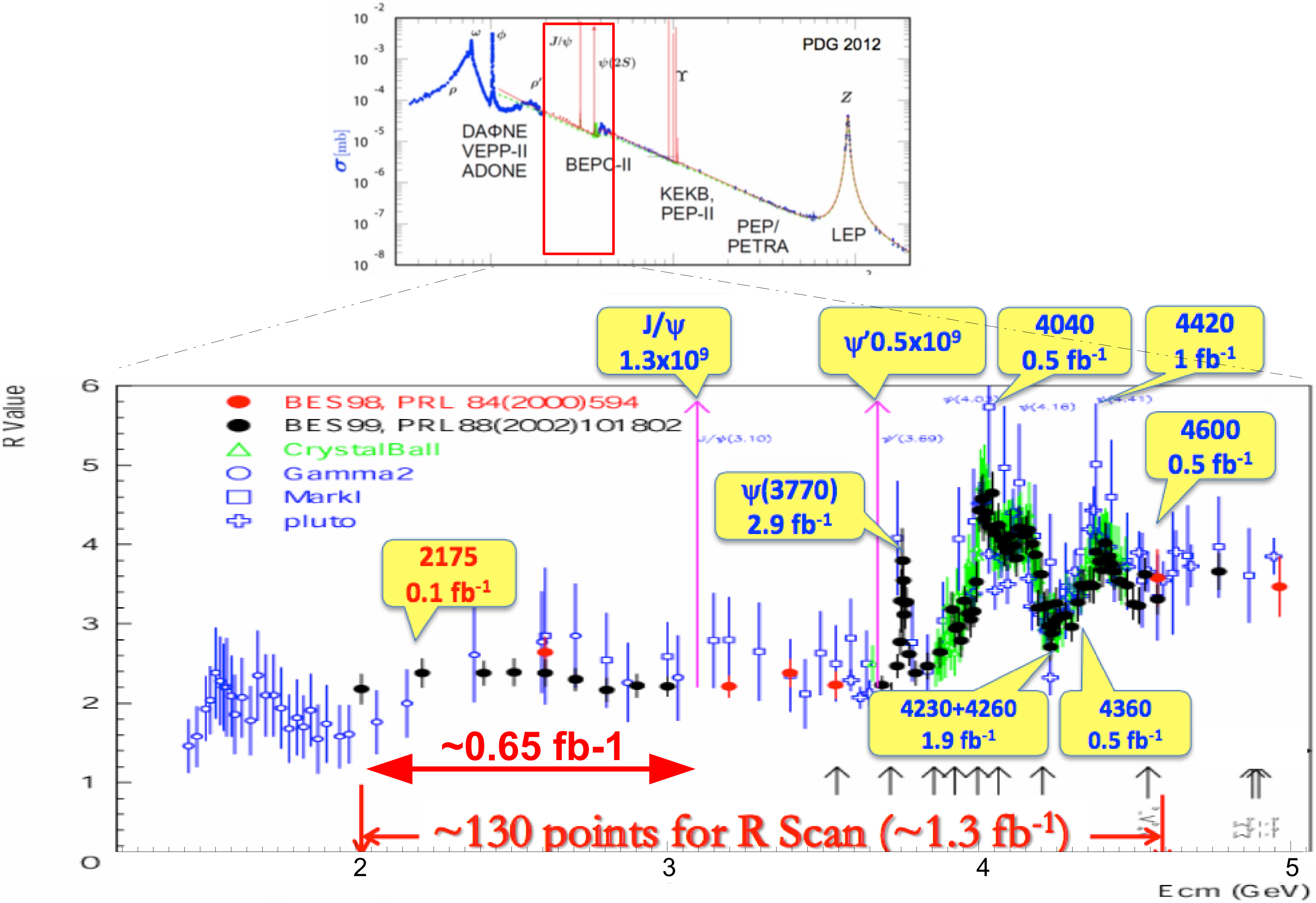

BESIII Data Samples for Nucleon FFs

In 2015 world largest scan data sample between 2 and 3.08 GeV!!

World largest J/Psi, Psi(2S), Psi(3770, Y(4260)...
produced directly in e+e- collisions

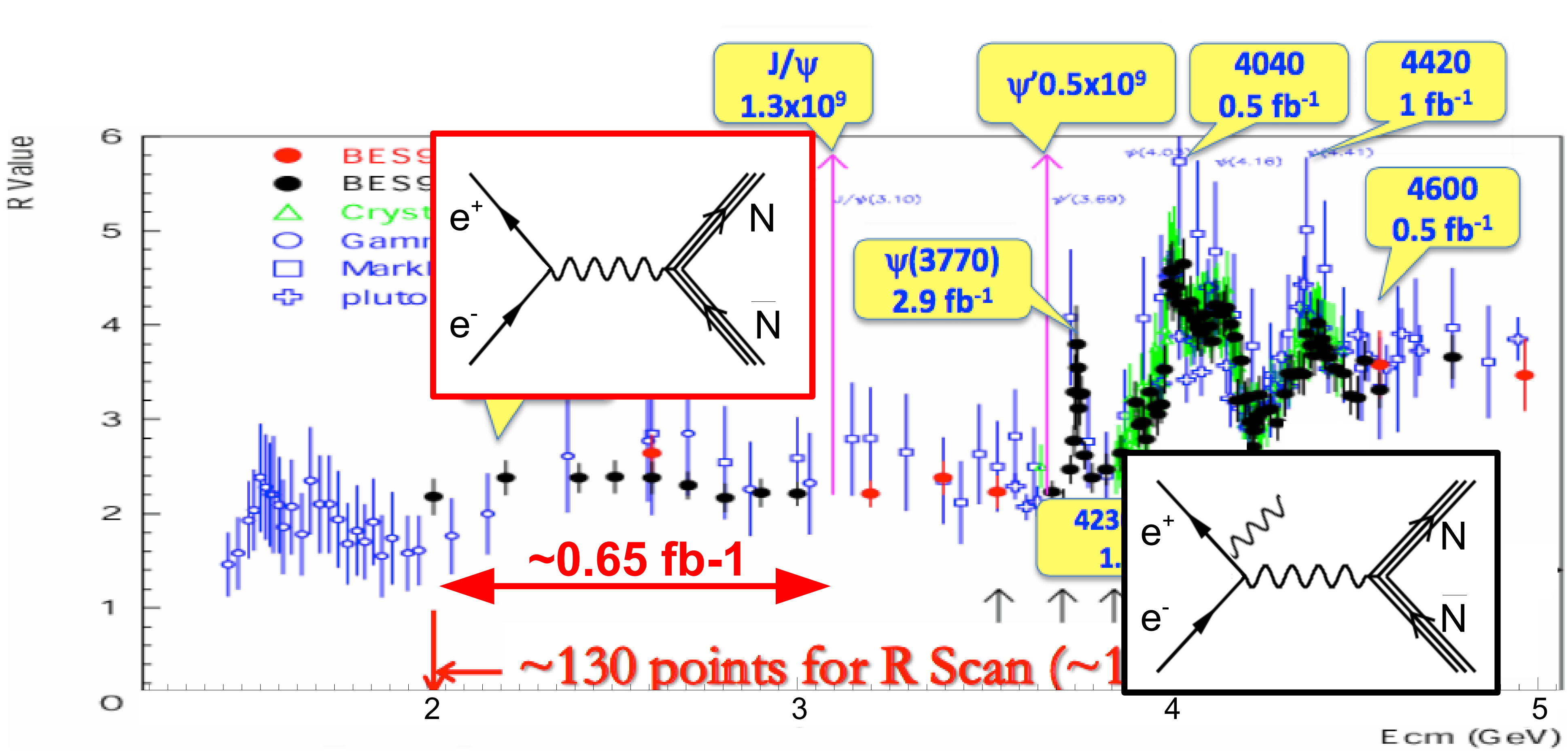

Physics program

[Int. J. Mod. Phys. A, Vol. 24 (2009)]

Light hadron physics

- Meson and baryon spetroscopy
- Multiquark states
- Threshold effects
- Glueballs and hybrids
- Two photon physics
- **Form factors**

QCD and τ

- Precision R measurement
- τ decays

Charmonium physics

- Precision spectroscopy
- Transitions and decays

Charm physics

- Semi-leptonic form factors
- Decay constants f_D and f_{Ds}
- CKM matrix: |Vcd|, |Vcs|
- Glueballs and hybrids
- $D0 - \overline{D0}$ mixing, CPV
- Strong phases

Precision mass measurements

- τ mass
- D, D* mass

XYZ meson physics

- Y(4260), Y(4360) properties
- Zc(3900)+...

Physics program

[Int. J. Mod. Phys. A, Vol. 24 (2009)]

Light hadron physics

- Meson and baryon spetroscopy
- Multiquark states

Charm physics

- Semi-leptonic form factors
- Decay constants f and f

- **Rich in resonanes**: charmonia and charmed mesons
- **Threshold characteristics** (pairs of τ, D, D_s, Λ_c...)
- **Transition region** between continuum and resonances, perturbative and non-perturbative QCD
- Location of **new hadrons**: glueballs, hybrids, multi-quark states

Charmonium physics

- Precision spectroscopy
- Transitions and decays

XYZ meson physics

- Y(4260), Y(4360) properties
- Zc(3900)+...

Nucleon EM Form Factors

Electro-magnetic Form Factors (FFs)

- **Spin ½ Baryons: two EM FFs**

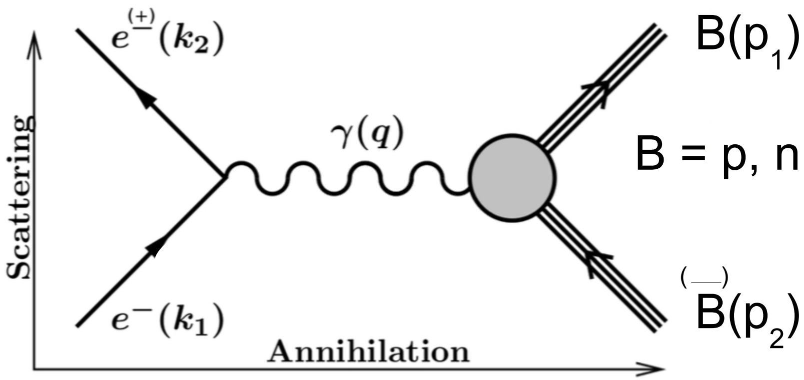

$$\Gamma^\mu(p_1,p_2) = \gamma^\mu \boldsymbol{F_1(q^2)} + \frac{i\sigma^{\mu\nu}q_\nu}{2M}\boldsymbol{F_2(q^2)}$$

$$F_1(0) = Q; F_2(0) = K$$

$$\boldsymbol{G_M(q^2)} = F_1(q^2) + F_2(q^2)$$

$$\boldsymbol{G_E(q^2)} = F_1(q^2) + \frac{q^2}{4M}F_2(q^2)$$

Space-like region

FFs real

Time-like region

FFs complex

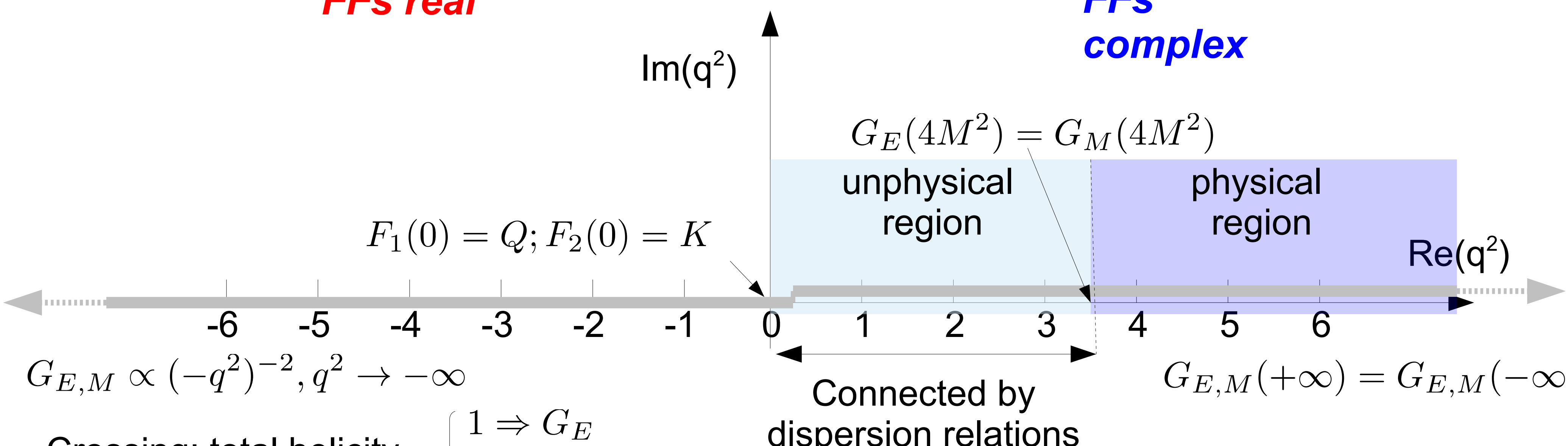

Crossing: total helicity $\begin{cases} 1 \Rightarrow G_E \\ 0 \Rightarrow G_M \end{cases}$

Time-like EM Form Factors (FFs)

- Experimental access: **angular distribution of Nucleon in e^+e^--center-of-mass**

Direct annihilation (fixed q^2, $q^2 \geq 0$): [Nuovo Cim. 24 (1962) 170]

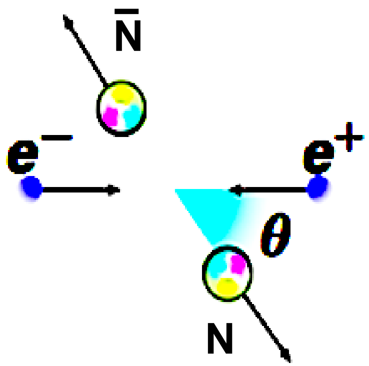

$$\frac{d\sigma^{Born,1\gamma}}{d\Omega} = \frac{\alpha^2 \beta C}{4q^2}\left[(1+\cos^2\theta)|G_M|^2 + \frac{4M^2}{q^2}\sin^2\theta |G_E|^2\right]$$

$$\sigma^{Born}(q^2) = \frac{4\pi\alpha^2\beta C}{3q^2}\left[|G_M(q^2)|^2 + \frac{2M^2}{q^2}|G_E(q^2)|^2\right]$$

Effective FF: $|G| = \sqrt{\frac{\sigma^{Born}(q^2)}{(1+\frac{2M^2}{q^2})(\frac{4\pi\alpha^2\beta C}{3q^2})}}$

C: Coulomb factor

Initial State Radiation ($4M^2 \leq q^2 \leq s$): [arXiv:1105.4975v2]

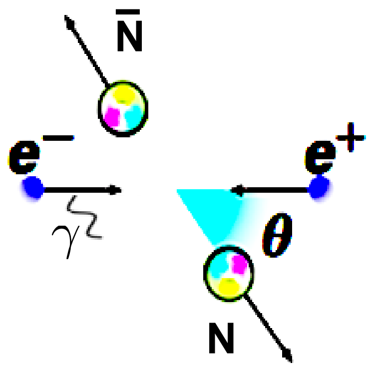

$$\frac{d^2\sigma^{ISR}}{dx\,d\theta_\gamma} = -W(s,x,\theta_\gamma)\sigma^{Born}(q^2)$$

$$W^{LO}(s,x,\theta_\gamma) = \frac{\alpha}{\pi x}\left(\frac{2-2x+x^2}{\sin^2\theta_\gamma} - \frac{x^2}{2}\right)$$

$$x = 1 - q^2/s = 2E_\gamma/\sqrt{s}$$

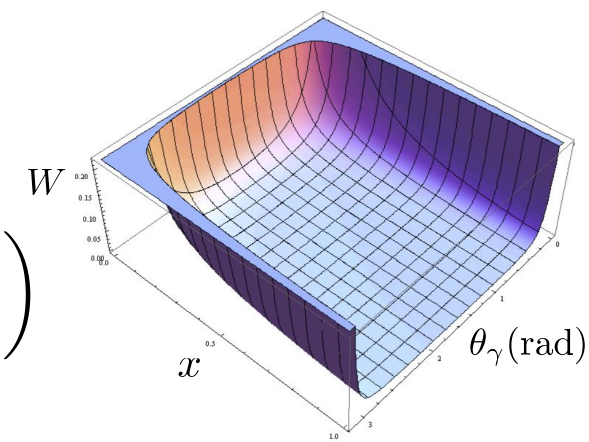

Time-like EM Form Factors (FFs)

- Experimental access: **angular distribution of Nucleon in e[+]e[-]-center-of-mass**

$\gamma\gamma$ exchange

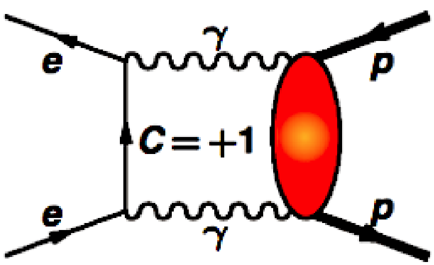

$\gamma\gamma$ exchange interfere with the Born term

Asymmetry in angular distributions

[PLB659, 197]

$$\frac{d\sigma^{Born,1\gamma}}{d\Omega} = \frac{\alpha^2\beta C}{4q^2}\left[(1+\cos^2\theta)|G_M|^2 + \frac{4M^2}{q^2}\sin^2\theta|G_E|^2\right]$$

$$\downarrow$$

$$\frac{d\sigma^{1\gamma\otimes 2\gamma}}{d\Omega} = \cos\theta\left[c_0(M^2_{p\bar{p}}) + c_1(M^2_{p\bar{p}})\cos^2\theta + c_2(M^2_{p\bar{p}})\cos^4\theta + \ldots\right]$$

$$\downarrow$$

$$\mathcal{A}(\cos\theta, M_{p\bar{p}}) = \frac{\frac{d\sigma}{d\Omega}(\cos\theta, M_{p\bar{p}}) - \frac{d\sigma}{d\Omega}(-\cos\theta, M_{p\bar{p}})}{\frac{d\sigma}{d\Omega}(\cos\theta, M_{p\bar{p}}) + \frac{d\sigma}{d\Omega}(-\cos\theta, M_{p\bar{p}})}$$

Also interference between ISR and FSR could cause an asymmetry!

Direct annihilation vs ISR

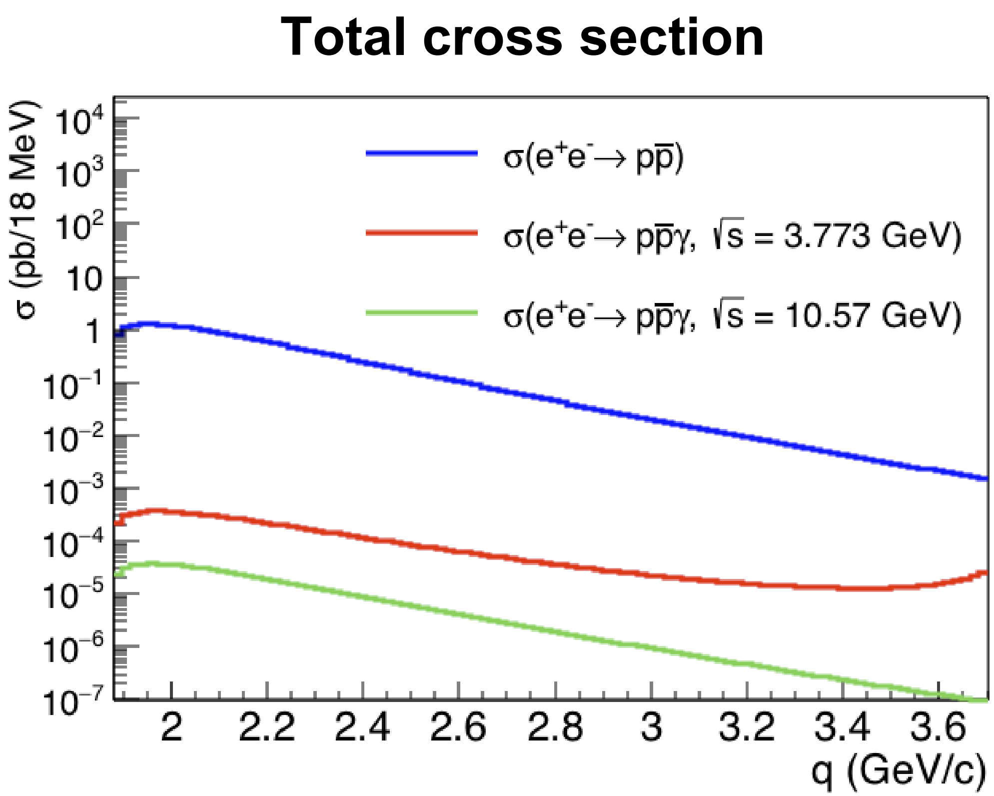

Direct annihilation vs Initial State Radiation

- High σ x low luminosity = high statistics
- High q^2 precision (ideal for $G_{E,M}$, thresholds, structure studies...)
- High geometrical acceptance of $N\bar{N}$ pair
- Low background

- Low σ x high luminosity = high statistics
- Continuous q^2-range available: $m^2_{th} < q^2 < s$ in one experiment
- Luminosity α bin width (low q^2 precision)
- Luminosity at threshold and acceptance != 0

Experimental situation: proton FFs

- First direct measurements of $\sigma_{Born}(ee \dashrightarrow p\bar{p})$ had poor statistics
  → only extraction of **effective form factor** possible

$$|G| = \sqrt{\frac{\sigma_{Born}}{(1+\frac{1}{2\tau})(\frac{4\pi\alpha^2\beta C}{3E_{CM}^2})}}$$

(Assumption: $|G| = |G_E| = |G_M|$)

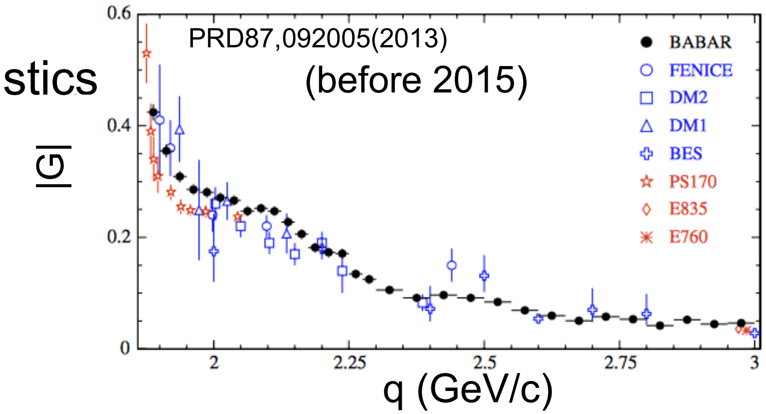

New measurements by BaBar (ISR) and $p\bar{p}$-experiments:

- Steep rise at threshold
- Steps near 2.25 and 3.0 GeV
- Asymptotic behavior in SL and TL regions differ:
  $|G_M^{TL}(10\ GeV^2)| > |G_M^{SL}(10\ GeV^2)|$

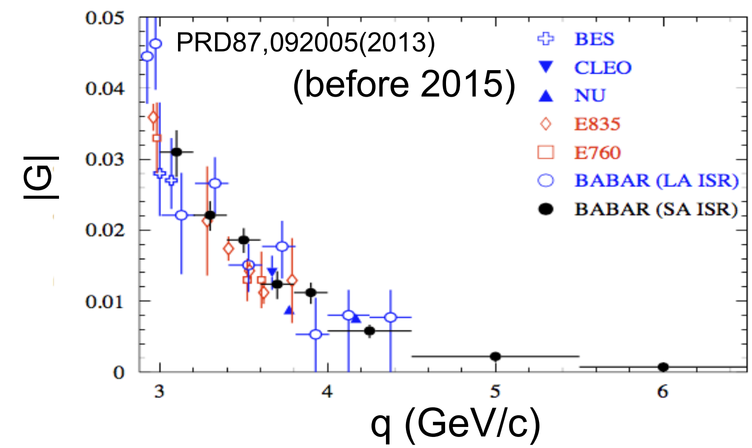

- Only BaBar and PS170 with statistics for angular analysis
  → extraction of **$R = |G_E| / |G_M|$** possible
  - Precision between 11% and 43%
  - Strong tension between Babar and PS170
  - No individual determination of $|G_E|$ and $|G_M|$

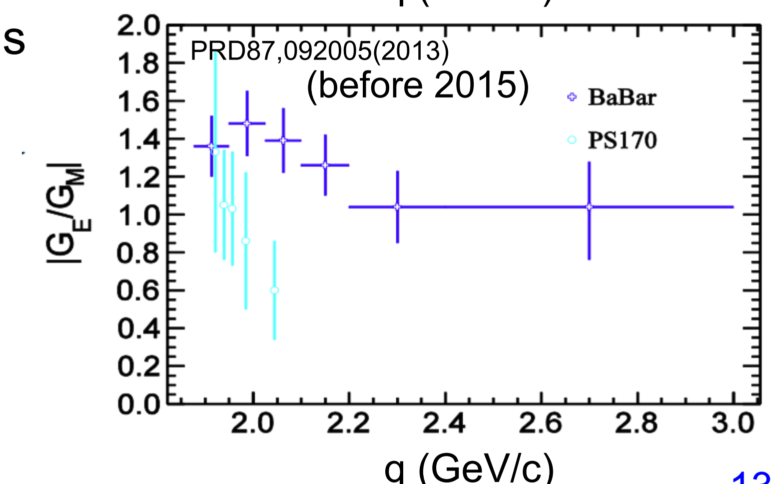

(Compilation of all experiments in backup slides)

Experimental situation: proton FFs

- Babar's statistics not enough to observe an asymmetry in the angular distribution

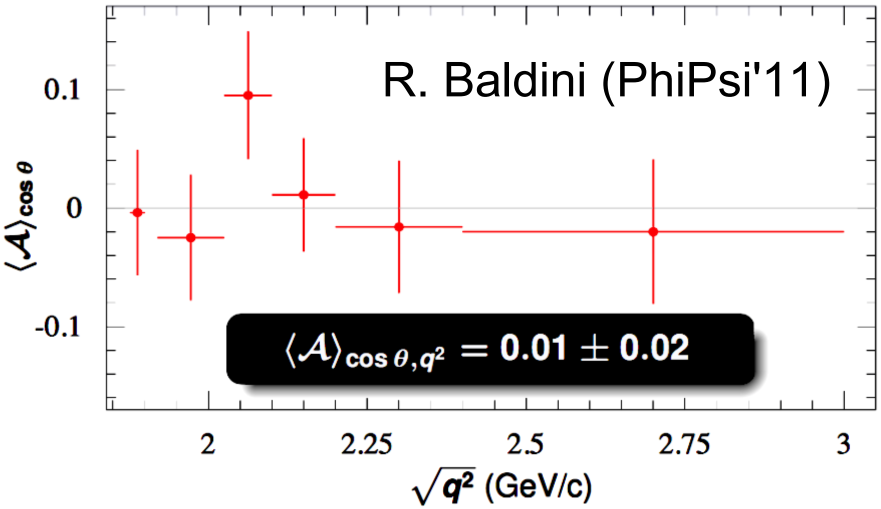

Being the integral asymmetry:

$$A_{\cos\theta_p} = \frac{\sigma(\cos\theta_p > 0) - \sigma(\cos\theta_p < 0)}{\sigma(\cos\theta_p > 0) + \sigma(\cos\theta_p < 0)}$$

$= -0.025 \pm 0.014 \pm 003$

- Periodic interference near threshold

[Phys. Rev. Lett. 114, 232301]

p = Proton momentum in p rest frame

Rescattering of proton and antiproton at low kinetic energy and distance ~1fm?

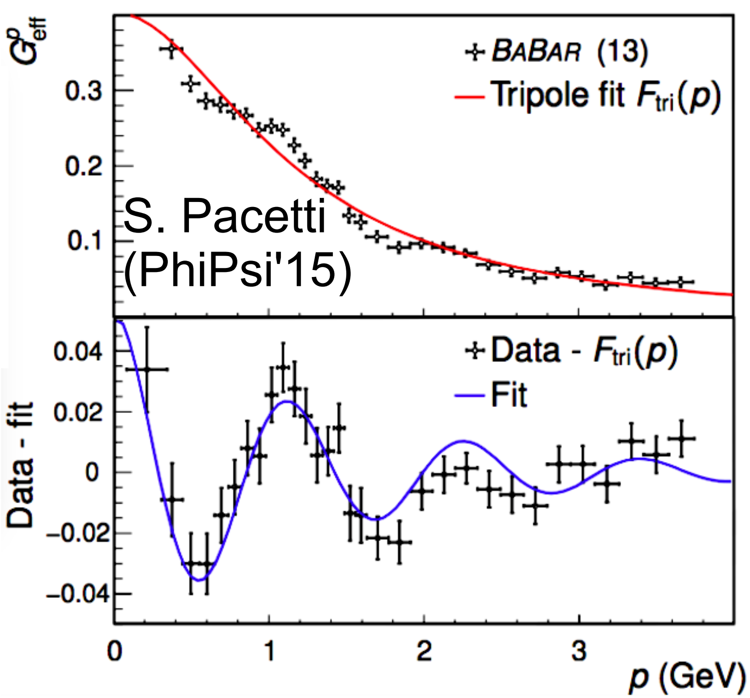

Experimental situation: neutron FFs

Only two direct measurements of $\sigma(e^+e^- \to n\bar{n})$ and neutron effective FF

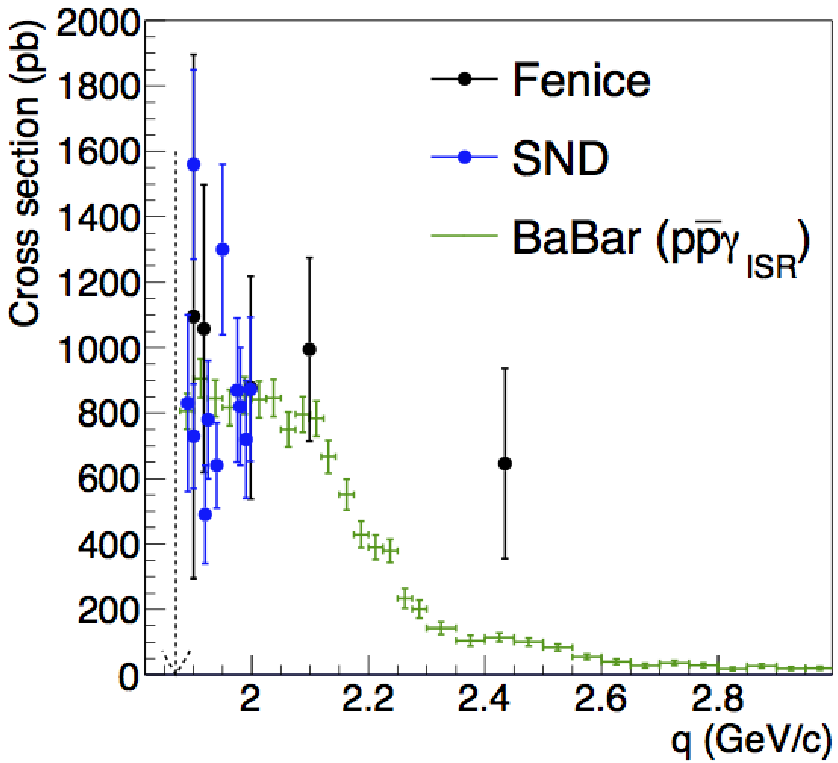

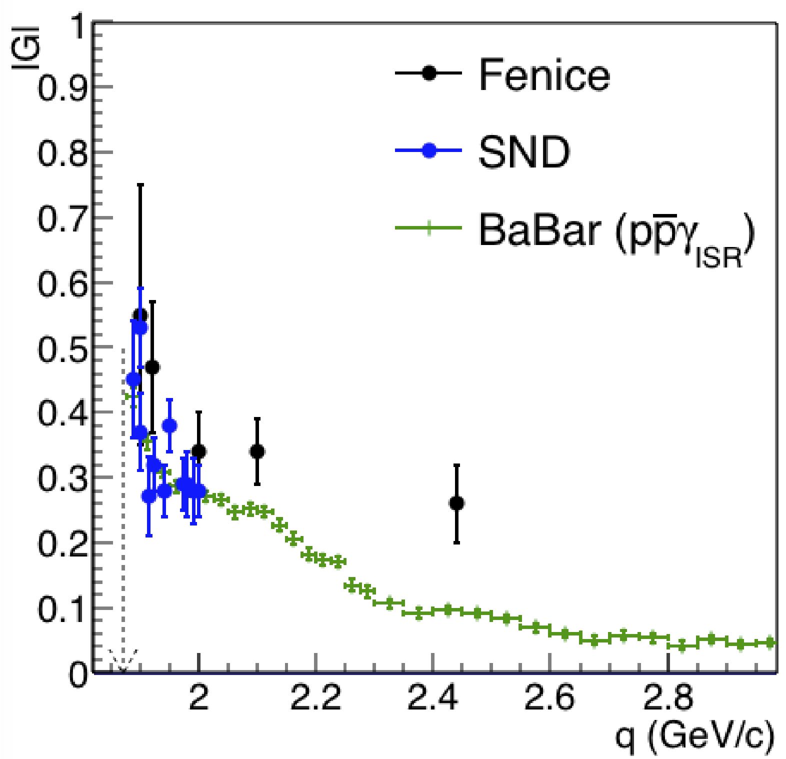

- At threshold cross section different from zero
- Close to threshold flat cross section and $\sigma(n\bar{n}) \approx \sigma(p\bar{p})$
- $|G^n|$ seems to be larger than $|G^p|$ as q increases (pQCD: $|G^p| = 2\cdot|G^n|$)
- No measurement of $R = |G_E/G_M|$ or $|G_E|$ and $|G_M|$ without previous assumption possible so far

Proton FFs from direct annihilation (scan)

Energy scan data samples

BESIII 2015: world largest scan samples between 2.0 and 3.08 GeV

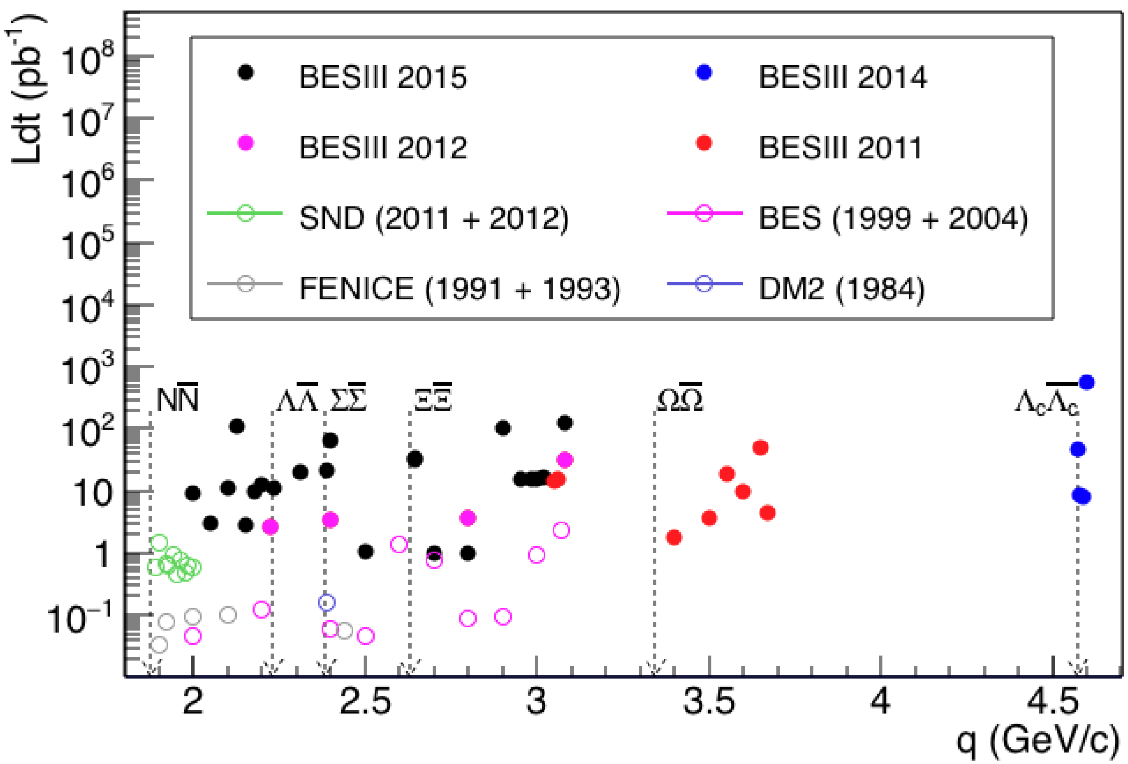

BESIII high luminosity scan 2015

E_{cm}(GeV)	L(pb^{-1})	E_{cm}(GeV)	L(pb^{-1})
2.0000	10.074	2.0500	3.343
2.1000	12.167	2.1250	108.49
2.1500	2.841	2.1750	10.625
2.2000	13.699	2.2324	11.856
2.3094	21.089	2.3864	22.549
2.3960	66.869	2.5000	1.098
2.6444	33.722	2.6464	34.003
2.7000	1.034	2.8000	1.008
2.9000	105.253	2.9500	15.942
2.9810	16.071	3.0000	15.881
3.0200	17.290	3.0800	126.185

- High accuracy in q^2 (Ffs, thresholds, structure studies...)
- High geometrical acceptance (detector coverage 93% of 4π)
- Low background contamination

$e^+e^- \rightarrow p\bar{p}$ Phys. Rev. D91, 112004 (2015)

Based on **157 pb^{-1}** collected in 12 scan points between **2.23 – 3.71 GeV** in 2011/2012

Event selection

- Good charged tracks:
  - |Rxy| < 1cm, |Rz| < 10 cm
  - |cos | < 0.93
- Particle identification
  - dE/dx + TOF
  - prob(p) > prob(K,)
  - For positive track: E/p < 0.5, cos <0.8
- Ntracks =2 & Np = N$\bar{p}$ =1
- $|tof_p - tof_{\bar{p}}| < 4ns$
- Angle between tracks
- Momentum window for p and $\bar{p}$

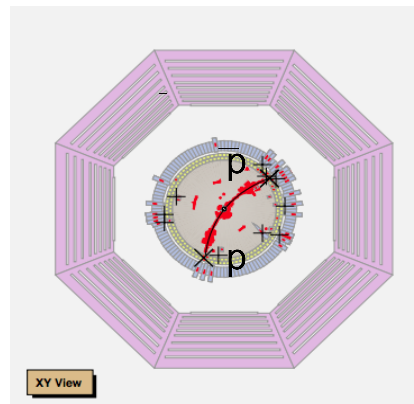

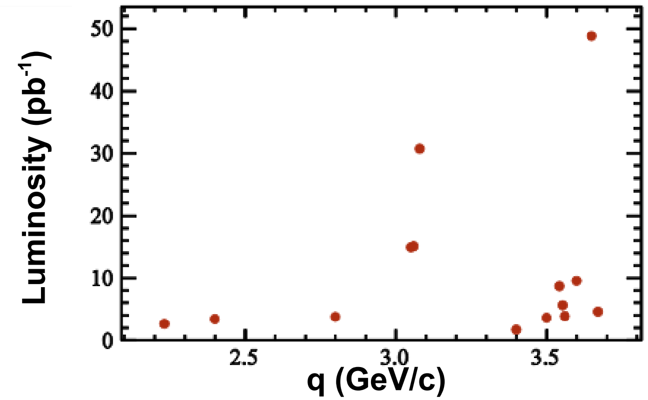

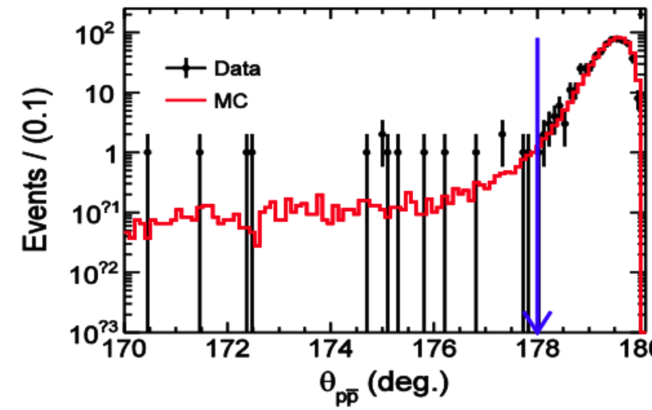

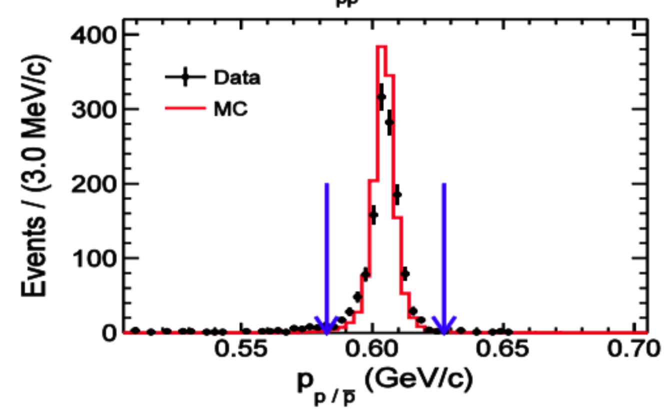

Background analysis

- Beam background: separated beam samples
- 2-body or multi-body with $p\bar{p}$ studied with MC

Negligible or subtracted ($\sqrt{s}$ > 3.0 GeV)

$e^+e^- \rightarrow p\bar{p}$ Phys. Rev. D91, 112004 (2015)

Extraction of $\sigma^{Born}(ee \rightarrow p\bar{p})$ and |G| for each scan point:

$$\sigma^{\mathrm{Born}}(q) = \frac{N_{\mathrm{obs}(q)} - N_{\mathrm{bg}(q)}}{L \cdot \epsilon(q) R(q)} \longrightarrow |G(q^2)| = \sqrt{\frac{\sigma^{\mathrm{Born}}(q^2)}{(1 + \frac{2M^2}{q^2})(\frac{4\pi\alpha^2\beta C}{3q^2})}}$$

- Efficiencies between 60% and 3% (ConExc)
- Radiative corrections up to LO in ISR (ConExc)
- Normalization to $e^+e^- \rightarrow e^+e^-$, $e^+e^- \rightarrow \gamma\gamma$ (Babayaga 3.5) [Phys.Lett.B520,16-24]

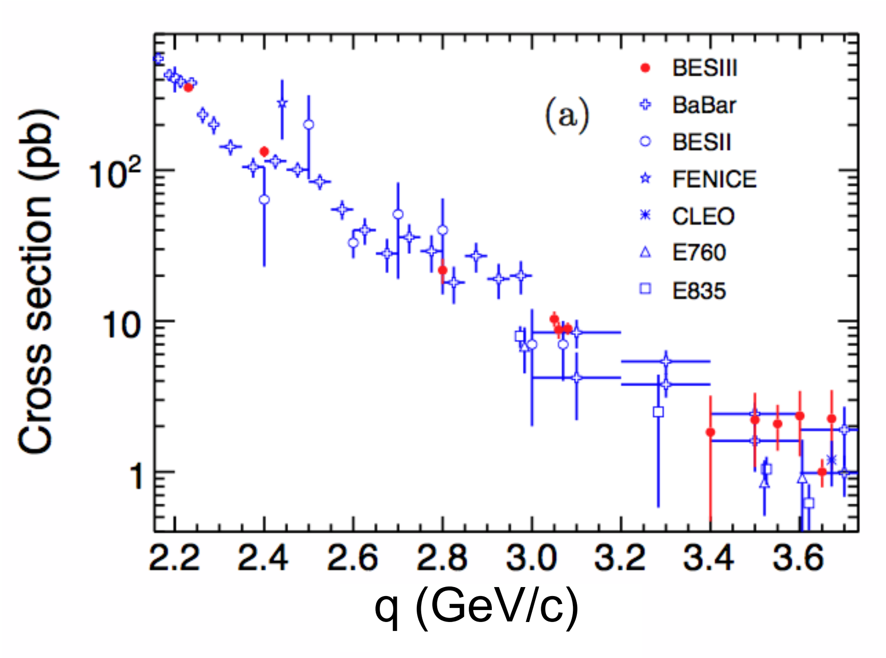

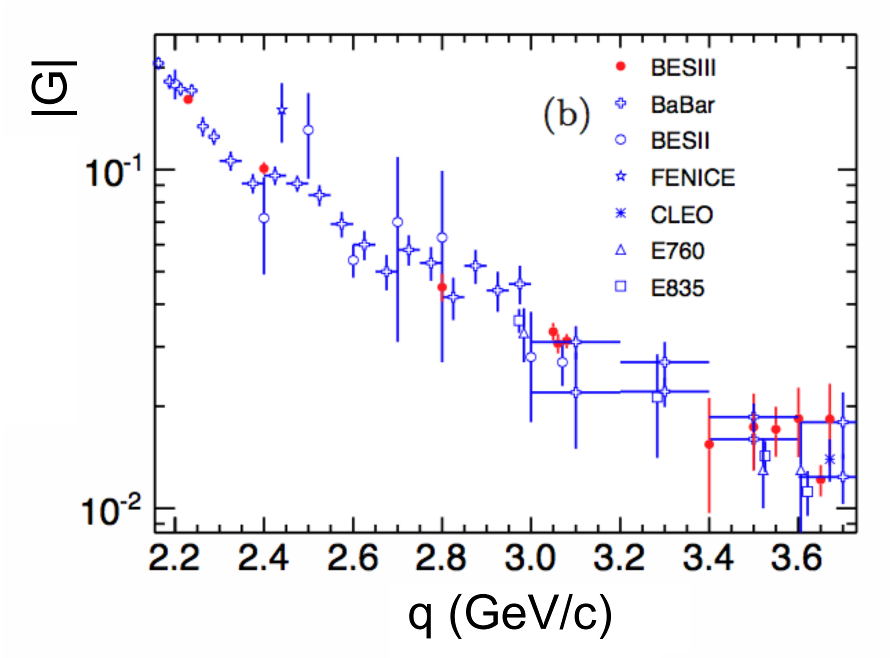

→ Overall uncertainty improved by 30%

Extraction of $R_{em} = |G_E/G_M|$ and $|G_M|$

- From **a 2-parameter fit** to the proton angular distribution in center-of-mass:

$$\frac{dN}{\epsilon \cdot (1+\delta) \cdot d\cos\theta_p} = N_{\rm norm} \cdot \boxed{|G_M|^2} \times \left[\frac{q^2}{4M_p^2} \cdot (1+\cos\theta_p^2) + \boxed{R^2} \cdot \sin\theta_p^2\right]$$

$$N_{norm} = \frac{2M_p^2 \cdot L \cdot \hbar c \cdot \pi\alpha^2 \cdot \beta C}{q^4}$$

- From the **measurement of the expectation value (method of moments)**:

$$<\cos^2\theta_p> = \frac{N_{norm} \cdot |G_M|^2}{N_{tot}} \int \epsilon \cdot (1+\delta) \cdot \left[\frac{q^2}{4M_p^2}(1+\cos^2\theta_p) + R_{em}^2 \sin^2\theta_p\right] d\cos\theta_p$$

For $\cos\theta_p$ within [-0.8,0.8]:

$$R = \sqrt{\frac{s}{4M_p^2} \frac{<\cos^2\theta_p> - 0.243}{0.108 - 0.648 <\cos^2\theta_p>}}$$

$$\sigma_R = \frac{0.0741}{R(0.167 - <\cos^2\theta_p>)^2} \frac{s}{4M_p^2} \sigma_{<\cos^2\theta_p>}$$

$|G_M|$ extracted from the integral of angular differential cross section and R

$e^+e^- \rightarrow p\bar{p}$ Phys. Rev. D91, 112004 (2015)

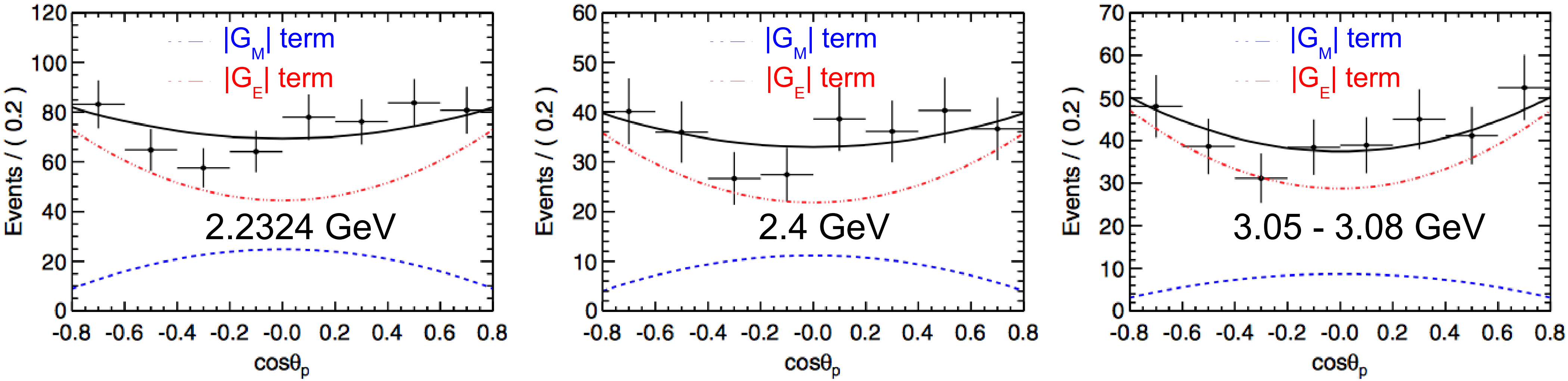

$\sqrt{s}$ (MeV)	$\lvert G_E/G_M \rvert$	$\lvert G_M \rvert$ ($\times 10^{-2}$)	χ^2/ndf
	Fit on $\cos\theta_p$		
2232.4	$0.87 \pm 0.24 \pm 0.05$	$18.42 \pm 5.09 \pm 0.98$	1.04
2400.0	$0.91 \pm 0.38 \pm 0.12$	$11.30 \pm 4.73 \pm 1.53$	0.74
(3050.0, 3080.0)	$0.95 \pm 0.45 \pm 0.21$	$3.61 \pm 1.71 \pm 0.82$	0.61
	method of moments		
2232.4	0.83 ± 0.24	18.60 ± 5.38	-
2400.0	0.85 ± 0.37	11.52 ± 5.01	-
(3050.0, 3080.0)	0.88 ± 0.46	3.34 ± 1.72	-

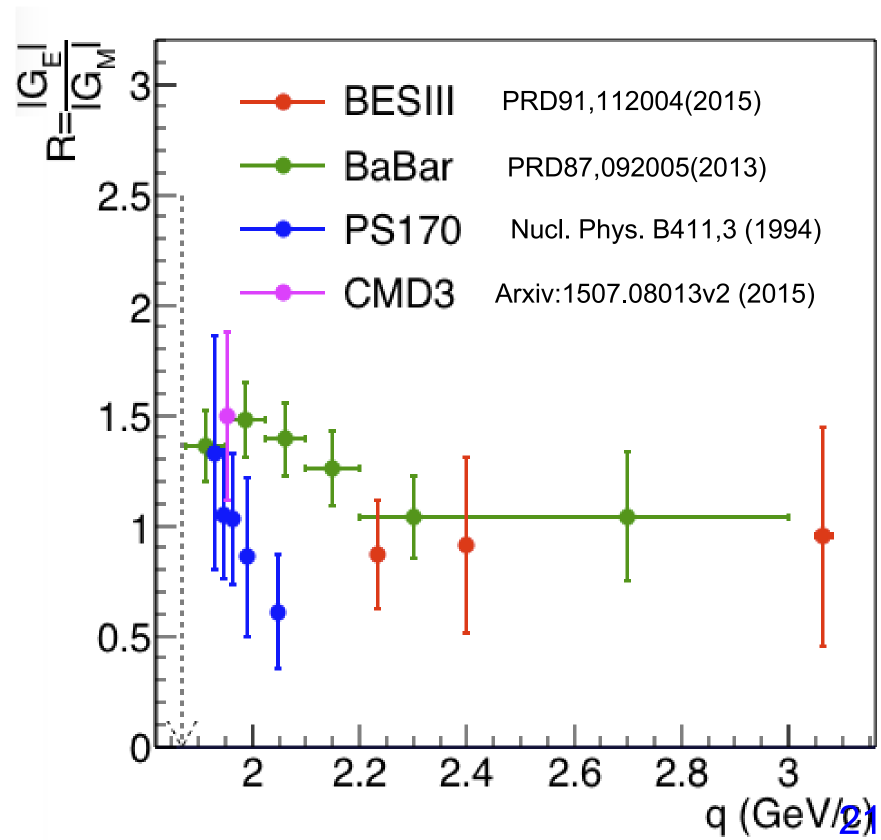

→ **$R = |G_E|/|G_M|$ consistent with 1**

→ **$|G_M|$ (and $|G_E|$) extracted for first time**

- Precision between 11% and 28%
- Strong tension between Babar and PS170

Prospects for $e^+e^- \rightarrow p\bar{p}$

About **650 pb^{-1}** collected in 22 scan points between **2.0 – 3.08 GeV** in 2015

Applying similar selection criteria as in previous analysis to MC samples of expected size, we expect:

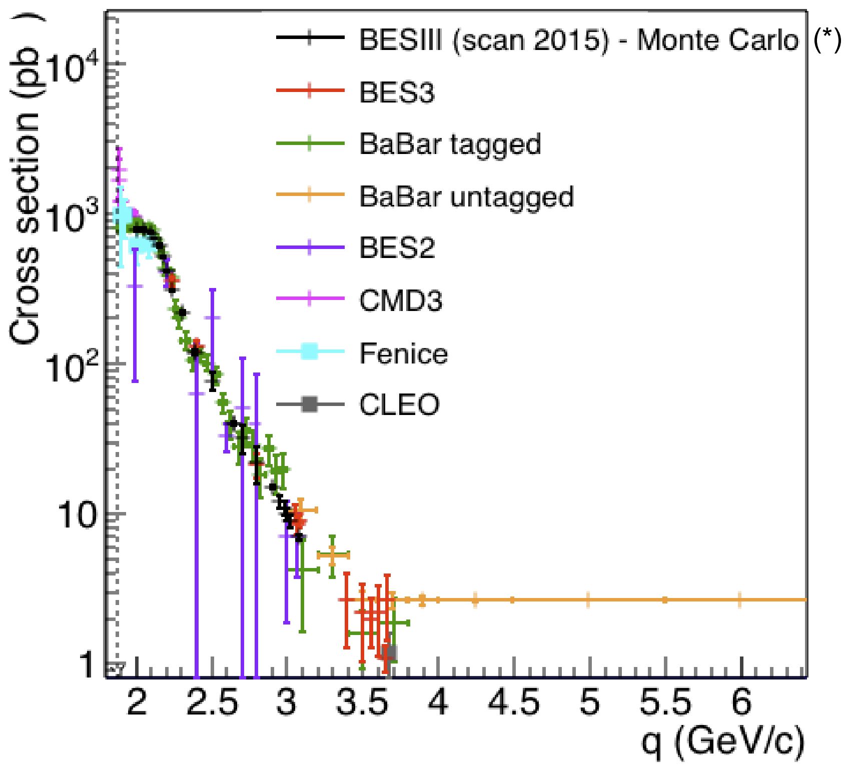

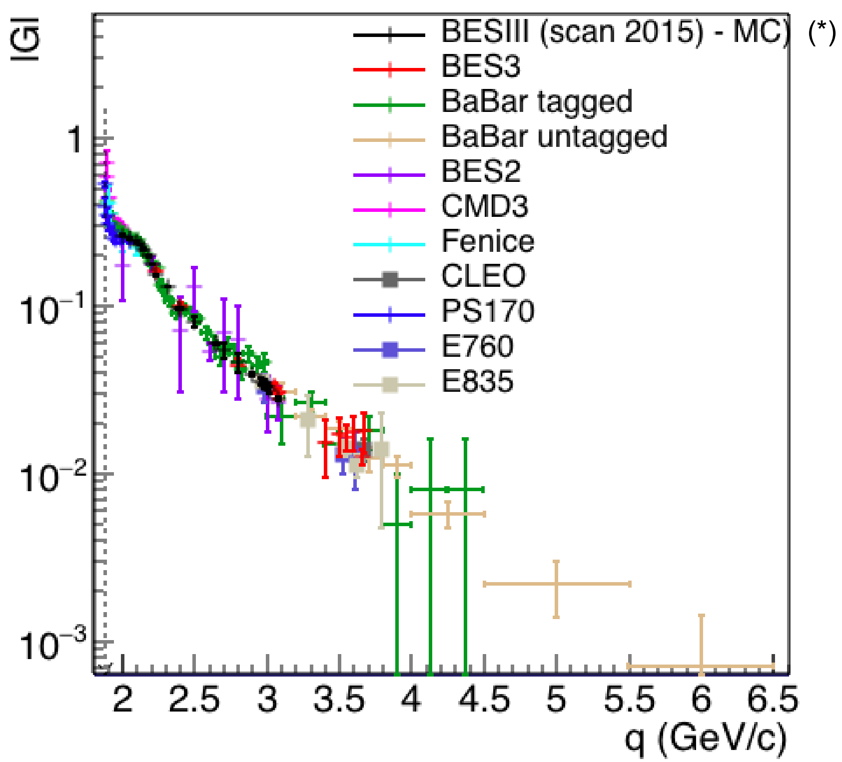

(*) Phokhara v9.1 [arXiv:1407.7995v2]. Default model based on BaBar's results.

Prospects for $e^+e^- \to p\bar{p}$: $\sigma(p\bar{p})$

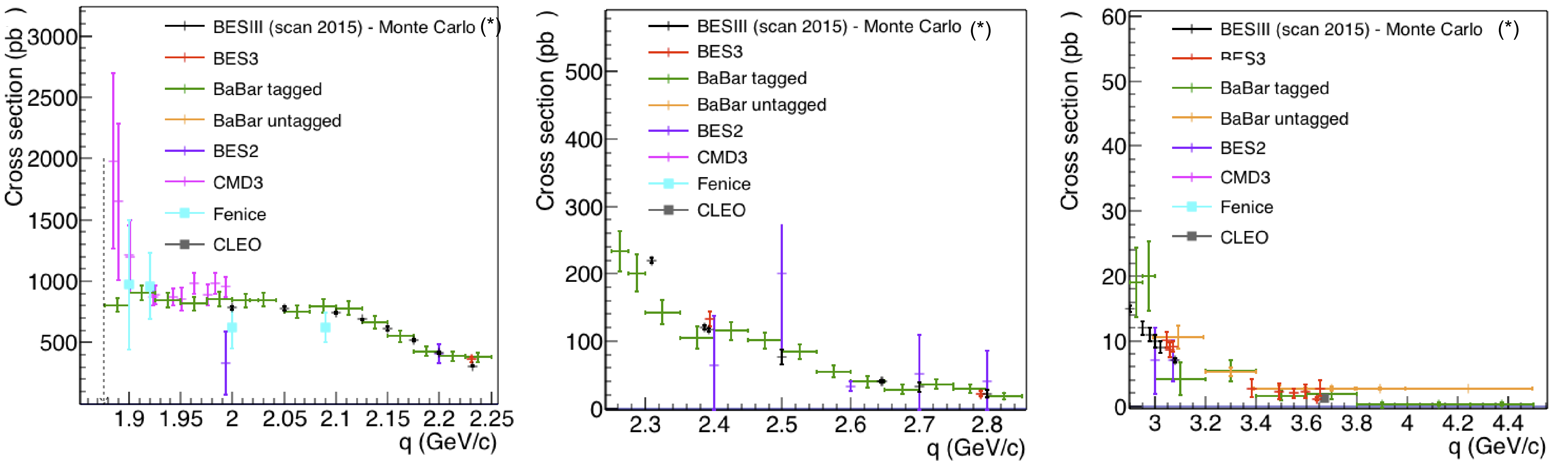

→ **Unprecedented accuracies above 2.0 GeV**
Expected accuracies **between 0.5%** (2.125 GeV) **and 26%** (2.8 GeV) and improving all measurements so far

→ Also data **samples collected around 'steps'** observed by BaBar (2.2 and 3.0 GeV) to check this observation

(*) Phokhara v9.1 [arXiv:1407.7995v2]. Default model based on BaBar's results.

Prospects for $e^+e^- \rightarrow p\bar{p}$: $\sigma(p\bar{p})$, $|G|$

$$|G(q^2)| = \sqrt{\frac{\sigma^{\mathrm{Born}}(q^2)}{\left(1+\frac{2M^2}{q^2}\right)\left(\frac{4\pi\alpha^2\beta C}{3q^2}\right)}}$$

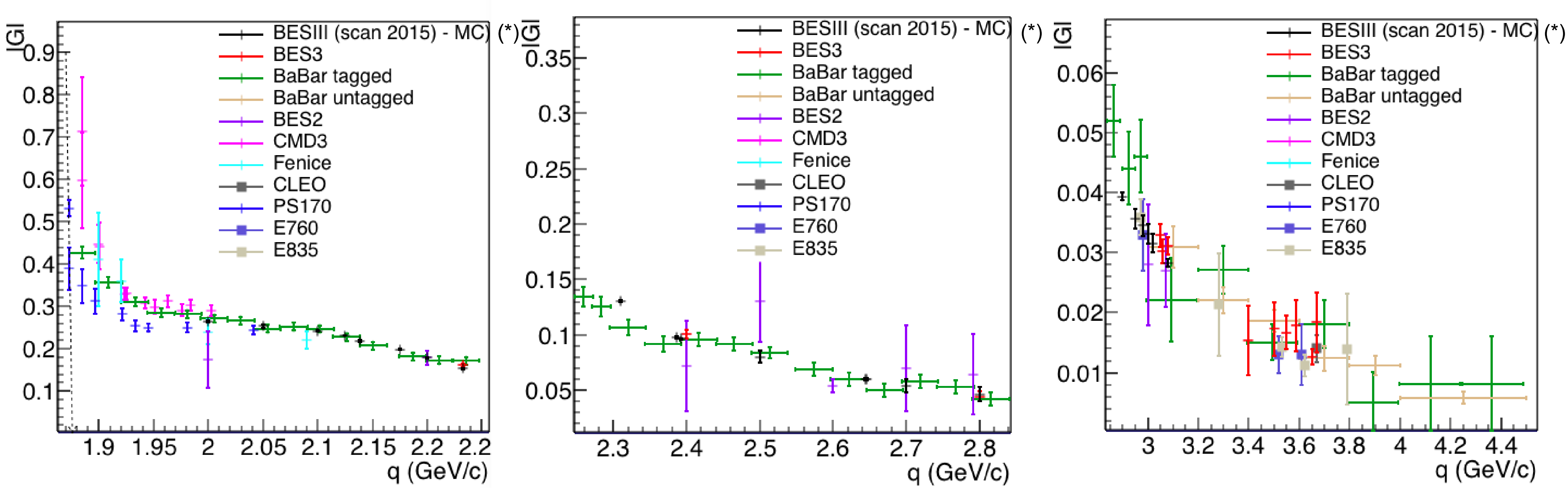

→ Expected accuracies **between 0.3%** (2.125 GeV) **and 13%** (2.8 GeV) and improving all measurements so far

(*) Phokhara v9.1 [arXiv:1407.7995v2]. Default model based on BaBar's results.

Prospects for $e^+e^- \rightarrow p\bar{p}$: R, $|G_{E,M}|$

16 scan points between 2.0 and 3.08 GeV with enough statistics for angular analysis:

Space-like

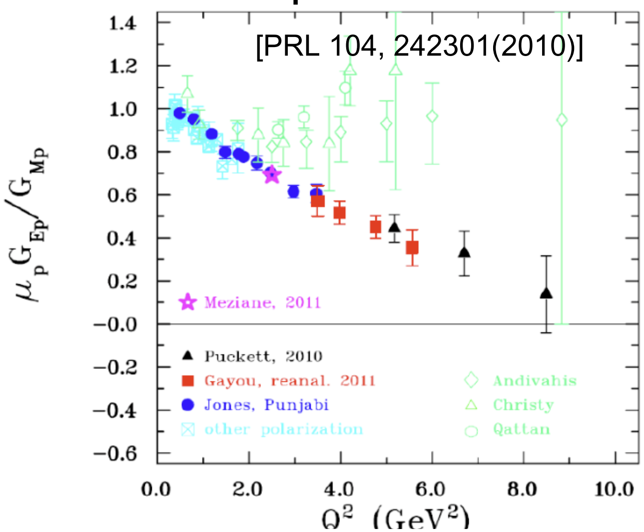

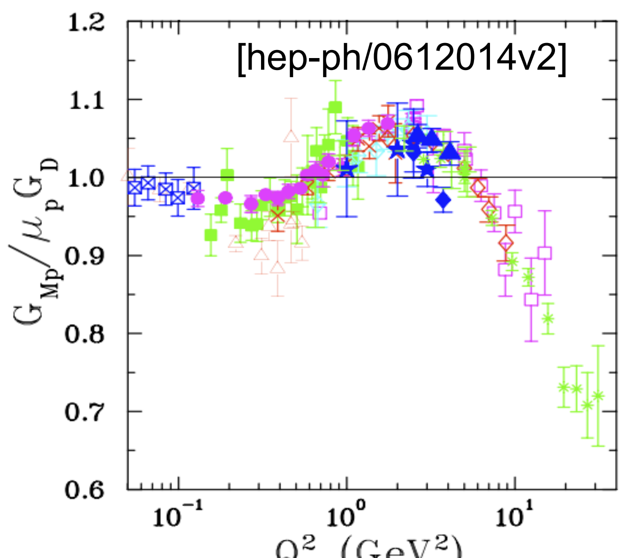

Time-like

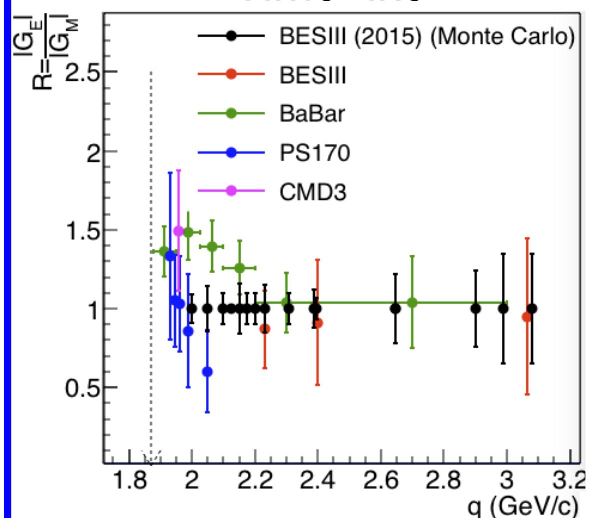

→ Expected **accuracies 3% to 35%**

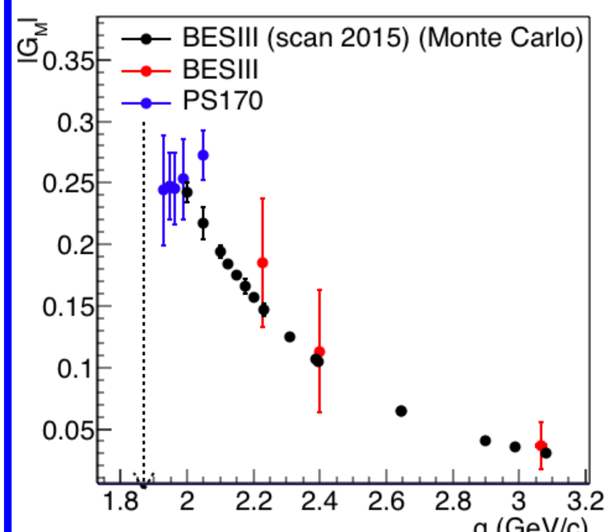

→ Expected **accuracies 1 to 9%** (3 to 35 % for $|G_E|$)

→ **Comparable accuracies in SL and TL regions for similar Q^2 values**

(*) Babayaga phase: modified Babayaga v3.5 with ppbar differential cross section for the ppbar channel with R=1 and $|G_m| = 22.5(1+q^2/0.71)^{-2} (1+q^2/3.6)^{-1}$ like in [Phys.Lett.B504,291]

Proton FFs from radiative return (ISR)

Data samples for $e^+e^- \to p\bar{p}\gamma_{ISR}$

BESIII: World largest Psi(3770), Psi(4040), Y(4260),Y(4360), Y(4420), Y(4600) produced directly in e+e- collisions

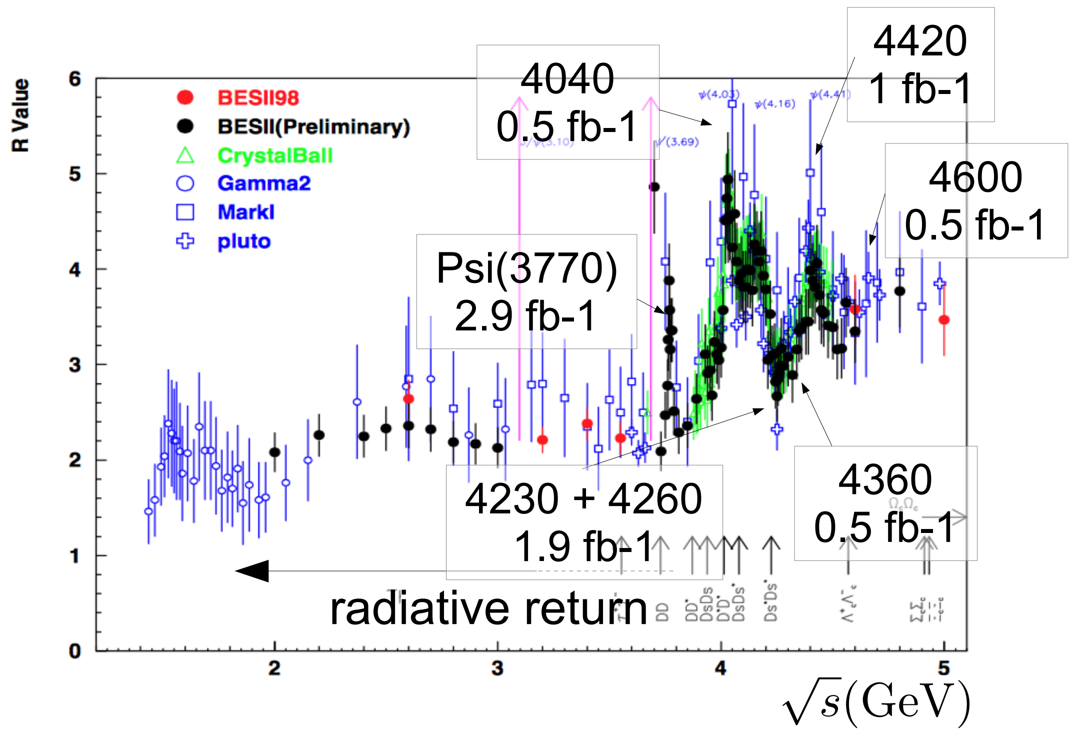

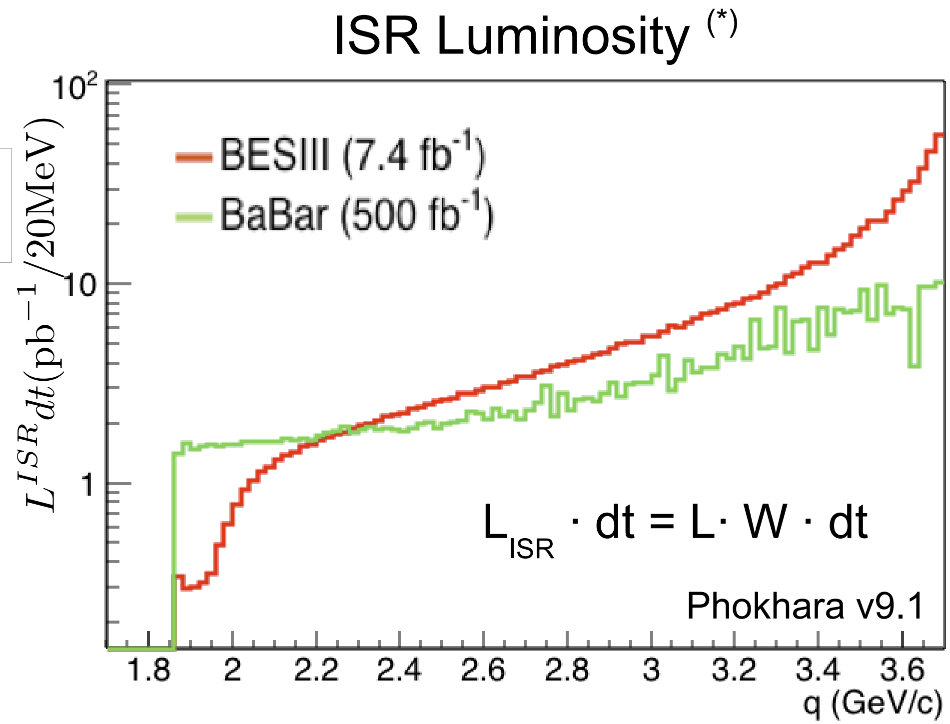

$e^+e^- \to p\bar{p}\gamma_{\rm ISR}$	BESIII	BaBar
$\sqrt{s}$ (GeV)	3.77 — 4.6	10.57
$\sigma^{\rm ISR}$ (nbarn)	$\sim 8 \times 10^{-3}$	$\sim 0.7 \times 10^{-3}$
$L(\mathrm{fb}^{-1})$	7.4	500
(*)$N\bar{N}$ in detector	50%	10%

→ **Similar statistics as BaBar** with much smaller luminosity!!

→ Why so little luminosity **at threshold?**

Data samples for $e^+e^- \to p\bar{p}\gamma_{ISR}$

BESIII: World largest Psi(3770), Psi(4040), Y(4260),Y(4360), Y(4420), Y(4600) produced directly in e+e- collisions

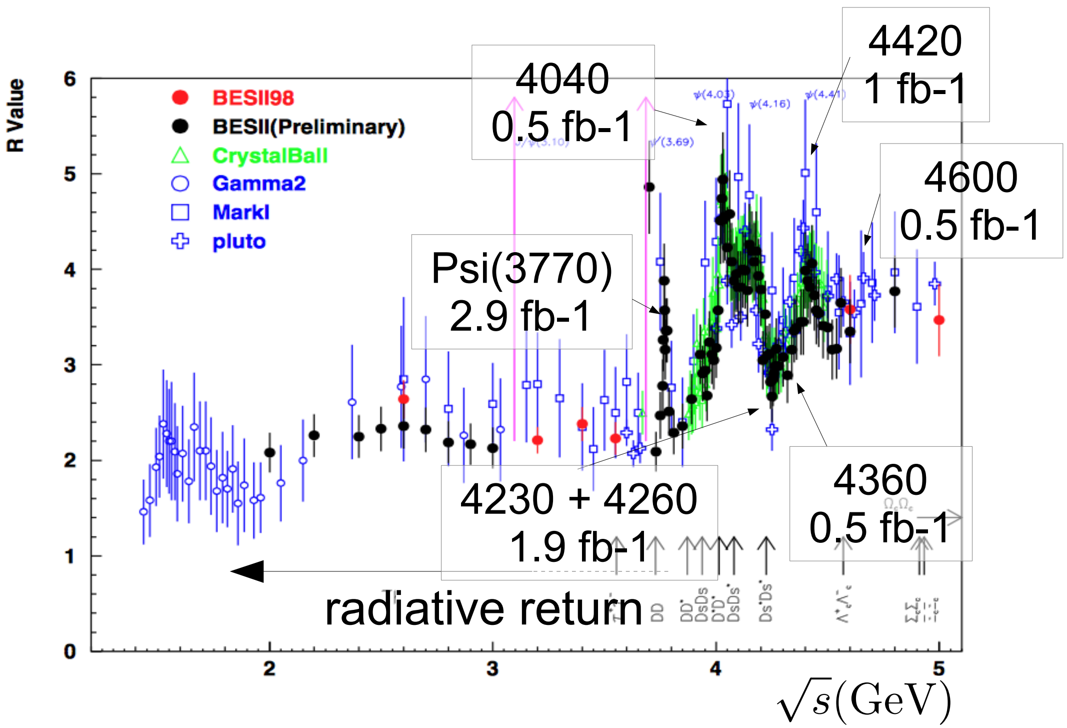

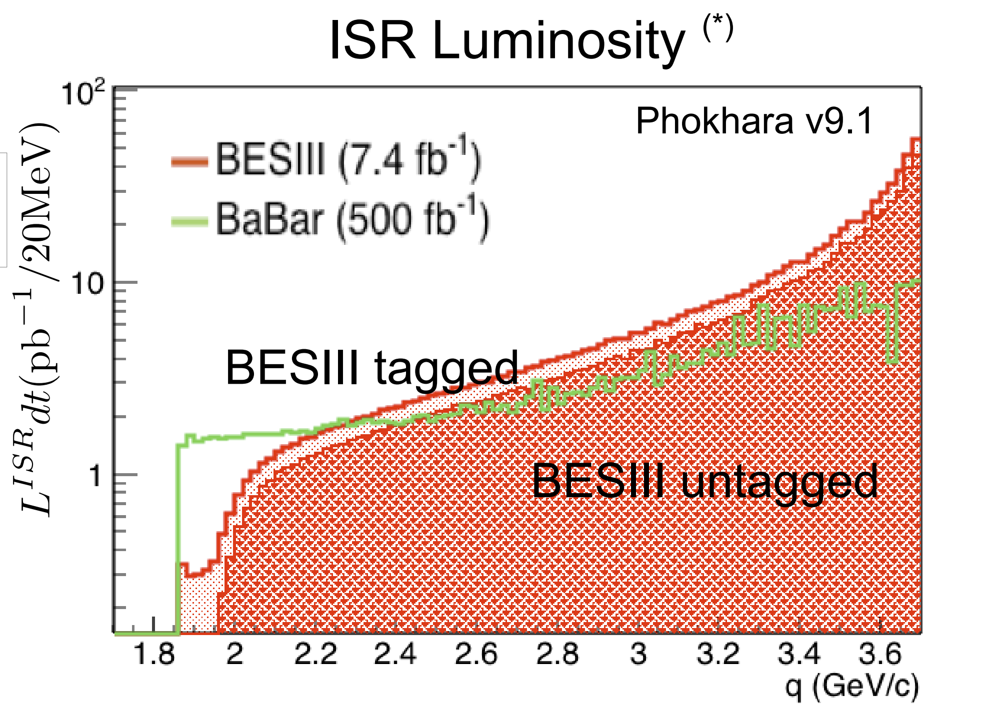

$e^+e^- \to p\bar{p}\gamma_{\text{ISR}}$	BESIII	BaBar
$\sqrt{s}$ (GeV)	3.77 — 4.6	10.57
σ^{ISR} (nbarn)	$\sim 8 \times 10^{-3}$	$\sim 0.7 \times 10^{-3}$
$L(\text{fb}^{-1})$	7.4	500
(*) $N\bar{N}$ in detector	50%	10%

→ **Similar statistics as BaBar** with much smaller luminosity!!

→ Why so little luminosity **at threshold? Only tagged photon analysis possible**

Properties of $e^+e^- \to p\bar{p}\gamma_{ISR}$

$\sqrt{s}(\mathrm{GeV})$ = 4.230 GeV, Phokhara v9.1 simulation [arXiv:1407.7995v2]

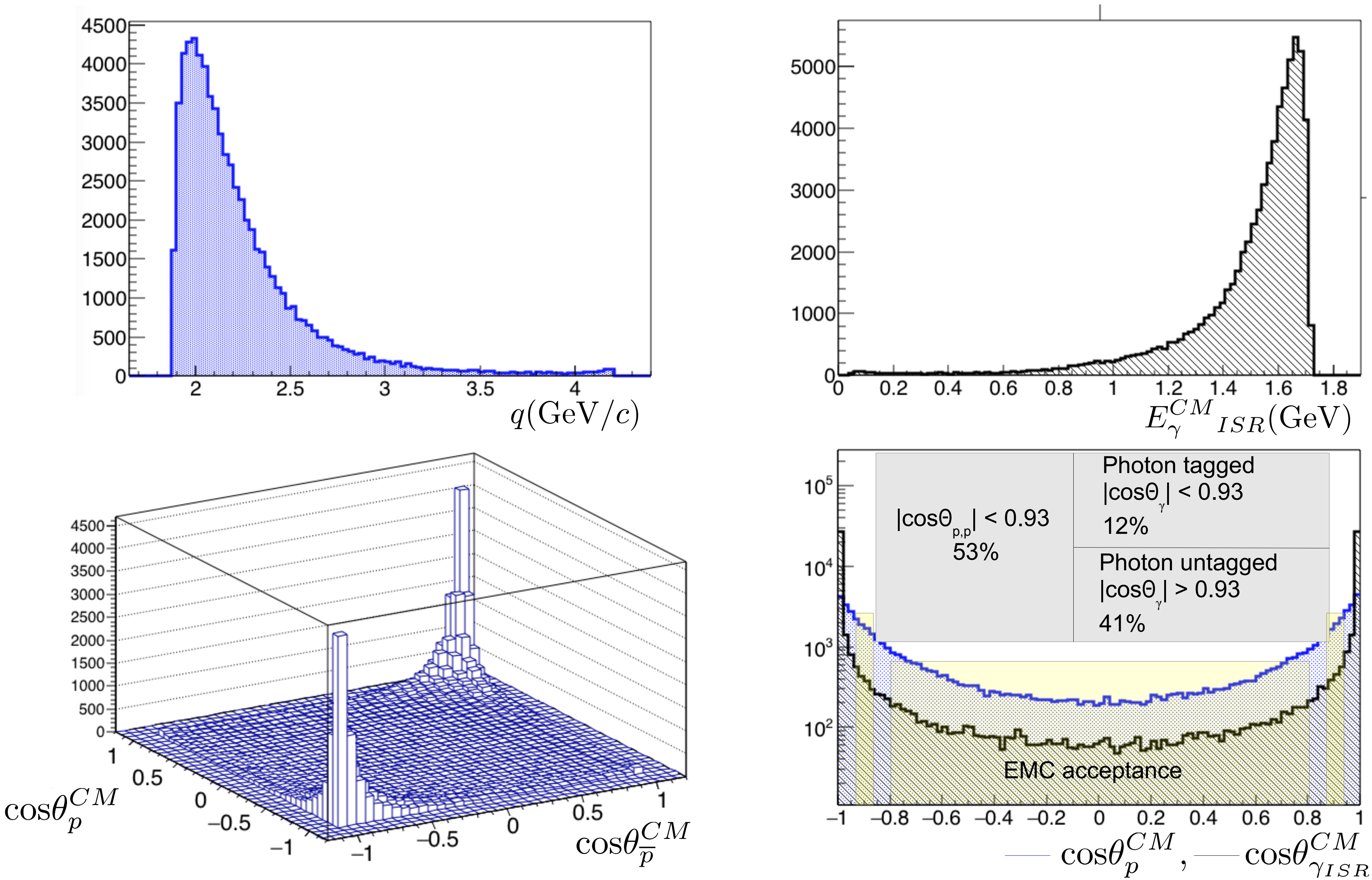

Analysis of $e^+e^- \to p\bar{p}\gamma_{ISR}$

Untagged γ_{ISR} analysis

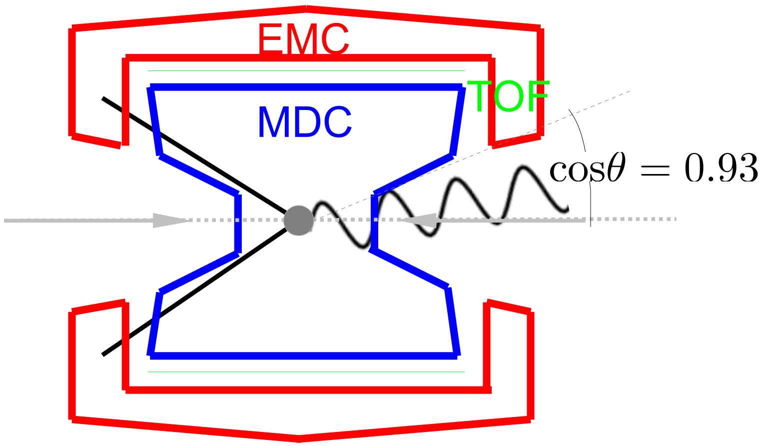

- **only $p\bar{p}$ reconstructed (41% of all events)**
- **identification of γ_{ISR} based on missing 4-momentum**

Tagged γ_{ISR} analysis

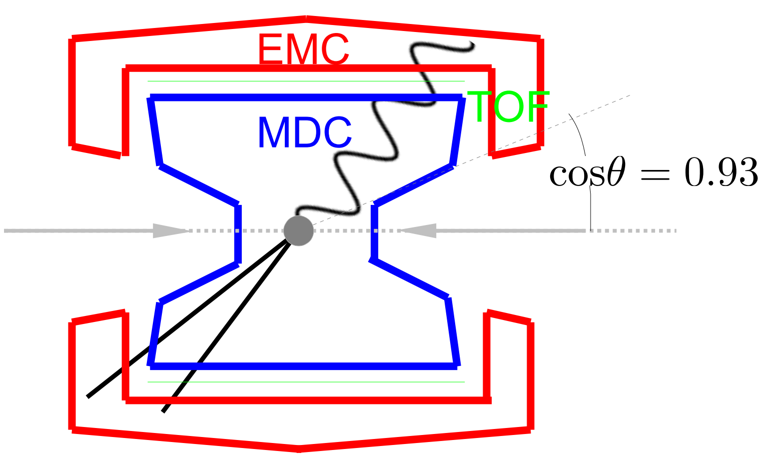

- **p, $\bar{p}$ and γ_{ISR} reconstructed (12% of all events)**

Analysis of $e^+e^- \to p\bar{p}\gamma_{ISR}$

Untagged $\gamma_{\rm ISR}$ analysis:

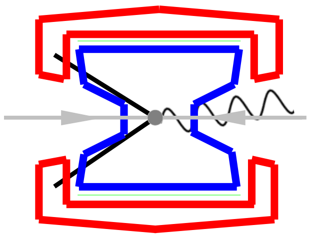

- **only $p\bar{p}$ reconstructed (41% of all events)**
- **identification of** $\gamma_{\rm ISR}$ **based on missing 4-momentum**

$$\vec{p}_{miss} = \vec{p}_p + \vec{p}_{\overline{p}} - \vec{p}_{e^+} - \vec{p}_{e^-} \to \theta_{miss}, |\vec{p}_{miss}| > 0.2 \mathrm{GeV/c}$$
$$M^2_{miss} = (p_p + p_{\overline{p}} - p_{e^+} - p_{e^-})^2$$

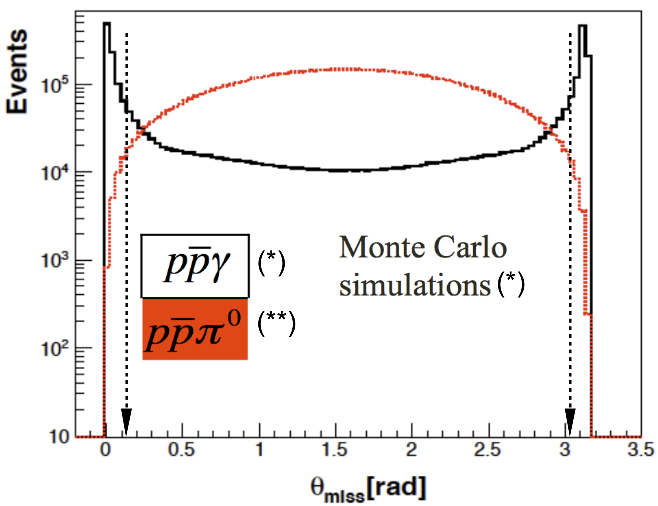

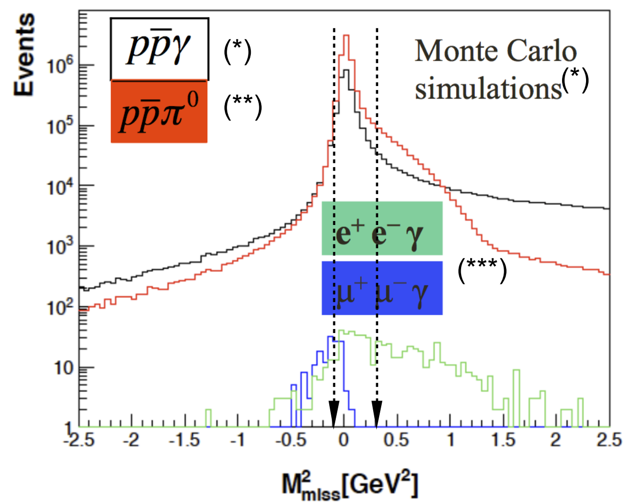

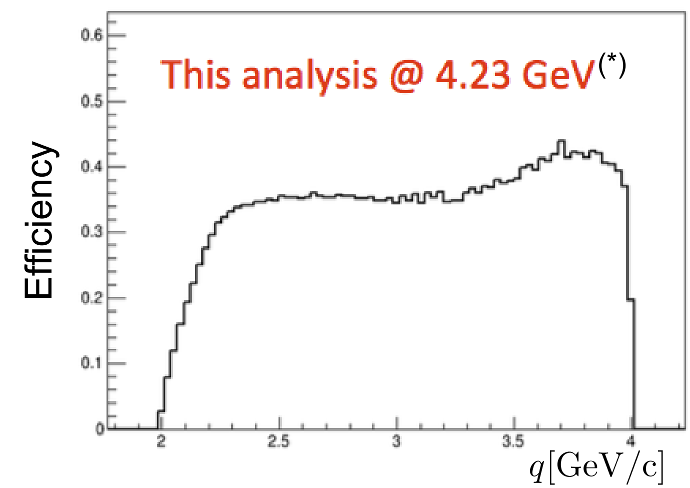

→ **Remaining ~2% background from** $e^+e^- \to p\bar{p}\pi^0$ **subtracted using sidebands**

→ **Signal efficiency increases with q and decreases with** $\sqrt{s}$

→ **Region accessible:** $2.0\mathrm{GeV} \leq q \leq 3.8\mathrm{GeV/c}$

(*) Phokhara v9.1 [arXiv:1407.7995v2]
(**) BesEvtGen [Chin.Phys. C32 (2008) 599]
(***) Babayaga 3.5

Analysis of $e^+e^- \to p\bar{p}\gamma_{ISR}$

Tagged $\gamma_{\rm ISR}$ analysis

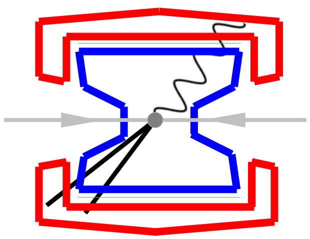

- **p, $\bar{p}$ and $\gamma_{\rm ISR}$ reconstructed (12% of all events)**
- **$\gamma_{\rm ISR}$ is the highest energetic shower in EMC (> 0.4 GeV)**
- **4-constraints kinematic fit to $e^+e^- \to p\bar{p}\gamma_{ISR}$**
- **π^0-veto: find π^0 and apply 5C kinematic fit to $e^+e^- \to p\bar{p}\pi^0$**

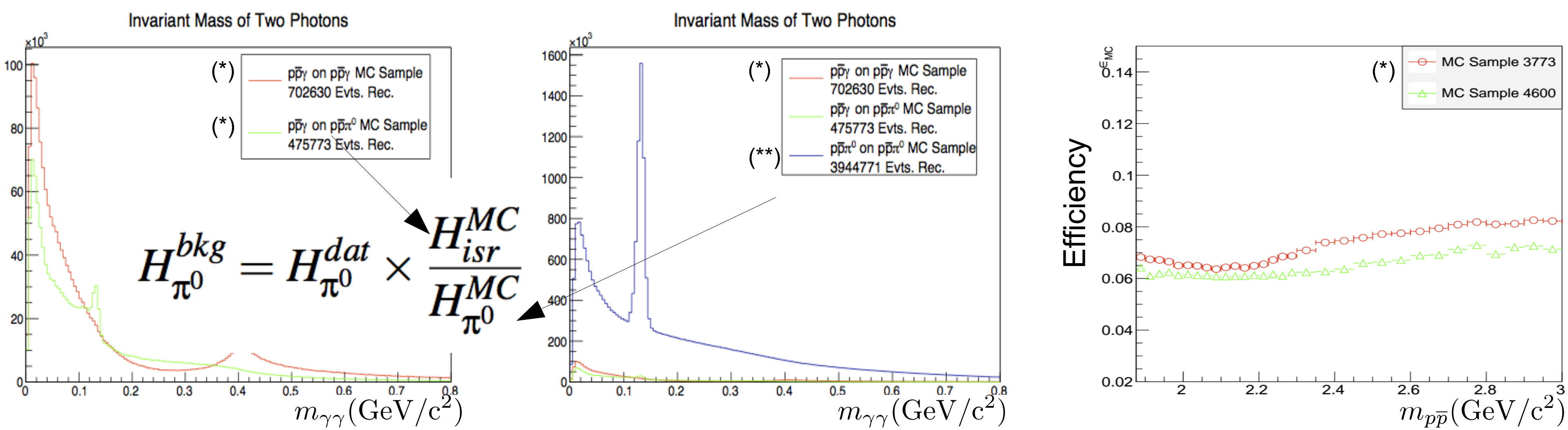

$$H^{bkg}_{\pi^0} = H^{dat}_{\pi^0} \times \frac{H^{MC}_{isr}}{H^{MC}_{\pi^0}}$$

→ **Remaining 20-60% background from $e^+e^- \to p\bar{p}\pi^0$ subtracted (MC weights)**

→ **Signal efficiency independent on q and decreasing slightly with $\sqrt{s}$**

→ **Region accessible: $2m_p \leq q \leq 3\mathrm{GeV}/c$**

(*) Phokhara v9.1 [arXiv:1407.7995v2]

(**) BesEvtGen [Chin.Phys. C32 (2008) 599]

Analysis of $e^+e^- \to p\bar{p}\gamma_{ISR}$

Data samples: ψ'',ψ(4040), Y(4230), Y(4260), Y(4360), Y(4420), Y(4600)

Total: 7.1 fb^{-1}

Analysis Strategy

$$\frac{dN_{i,p\bar{p}\gamma_{ISR}}(q)}{dq}$$

Efficiencies, background, radiative factor, (functions dependent on q)

For each data sample (i): tagged and untagged analysis

Add all corrected data from different $\sqrt{s}$ for each q-bin → $N_{p\bar{p}\gamma}(q) = \sum_i \frac{N_i^{obs}(q) - N_i^{bg}(q)}{\epsilon_i(q) R_i(q)}$

Normalize with L_{ISR} → $L^{ISR}(q) = \sum_i L_i^{ISR}(q)$

Born cross section, Effective form factor → $\sigma_{p\bar{p}}(q) = \frac{N_{p\bar{p}\gamma}(q)}{L^{ISR}(q)}$

Angular analysis: **Extraction of R** → In $p\bar{p}$-frame:

$$\frac{dN}{d\cos\theta_p} = A[H_M(\cos\theta_p, q) + \frac{|G_E|^2}{|G_M|^2} H_E(\cos\theta_p, q)]$$

Prospects for $e^+e^- \rightarrow p\bar{p}\gamma_{ISR}$: $\sigma(p\bar{p})$, $|G|$

Untagged $\gamma_{\rm ISR}$ analysis:

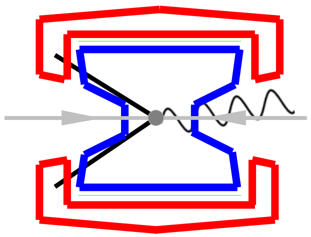

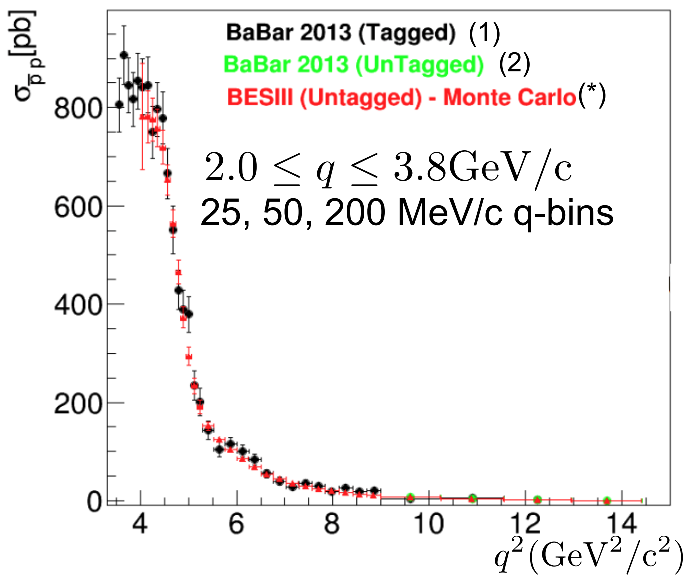

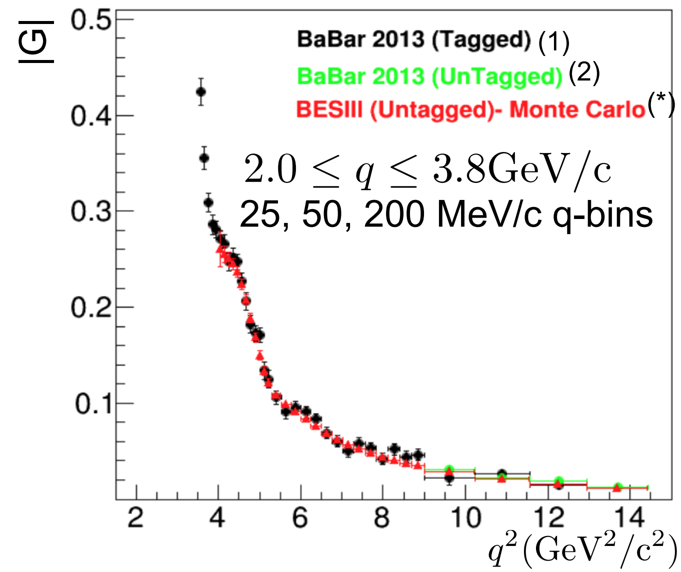

→ **Final statistics competitive with BaBar**

(1) PRD87,092005(2013)
(2) PRD88,072009(2013)

Tagged $\gamma_{\rm ISR}$ analysis:

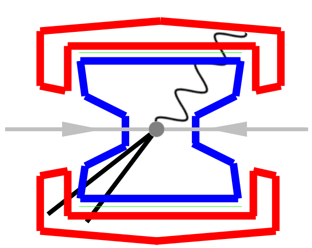

→ **Cross section and effective form factor measured between threshold and 3.0 GeV** in same q-bin sizes as untagged analysis

→ Expected about **3 times less statistics than for untagged** case

(*) Phokhara v9.1 [arXiv:1407.7995v2]

Prospects for $e^+e^- \to p\bar{p}\gamma_{ISR}$: $R = |G_E|/|G_M|$

Angular analysis in q-intervals:

$$\frac{dN}{d\cos\theta_p} = A[\underbrace{H_M(\cos\theta_p, q)}_{\text{from MC with } |G_E|=0} + \frac{|G_E|^2}{|G_M|^2}\underbrace{H_E(\cos\theta_p, q)}_{\text{from MC with } |G_M|=0}]$$

Two methods used: 2parametrs fit and method of moments

Untagged $\gamma_{\rm ISR}$ analysis:

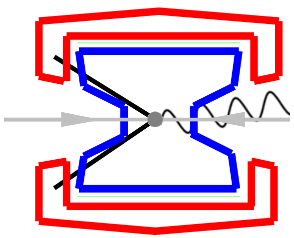

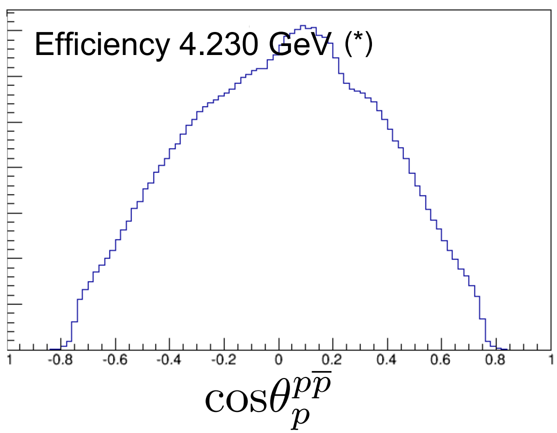

Extraction of R at 4 q-intervals possible

[2.0-2.2[,[2.2-2.4[,[2.4-2.6[,[2.6-3.0[

→ **Expected stat. accuracies ~30%**

Tagged $\gamma_{\rm ISR}$ analysis

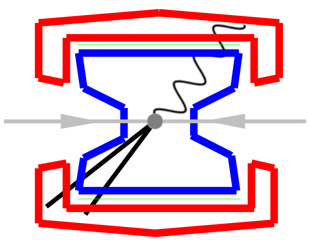

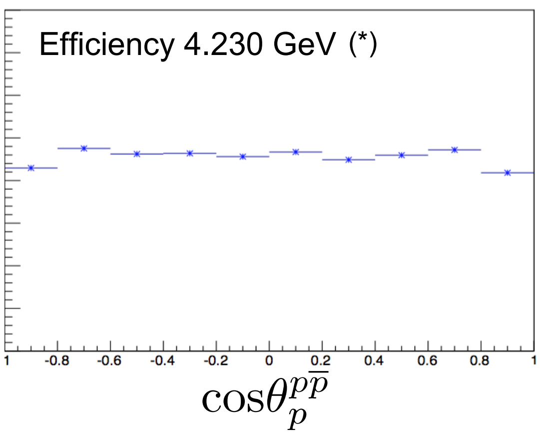

Extraction of R at 6 q-intervals possible:

[1.876-1.950[,[1.950-2.025[,
[2.025-2.1[,[2.1-2.2[,[2.2-2.4[,[2.4-3.0[

→ **Expected stat. accuracies between 20% and 65% (as q increases)**

(*) Phokhara v9.1 [arXiv:1407.7995v2]

Neutron FFs from direct annihilation (scan)

Detection of Neutrons in BESIII

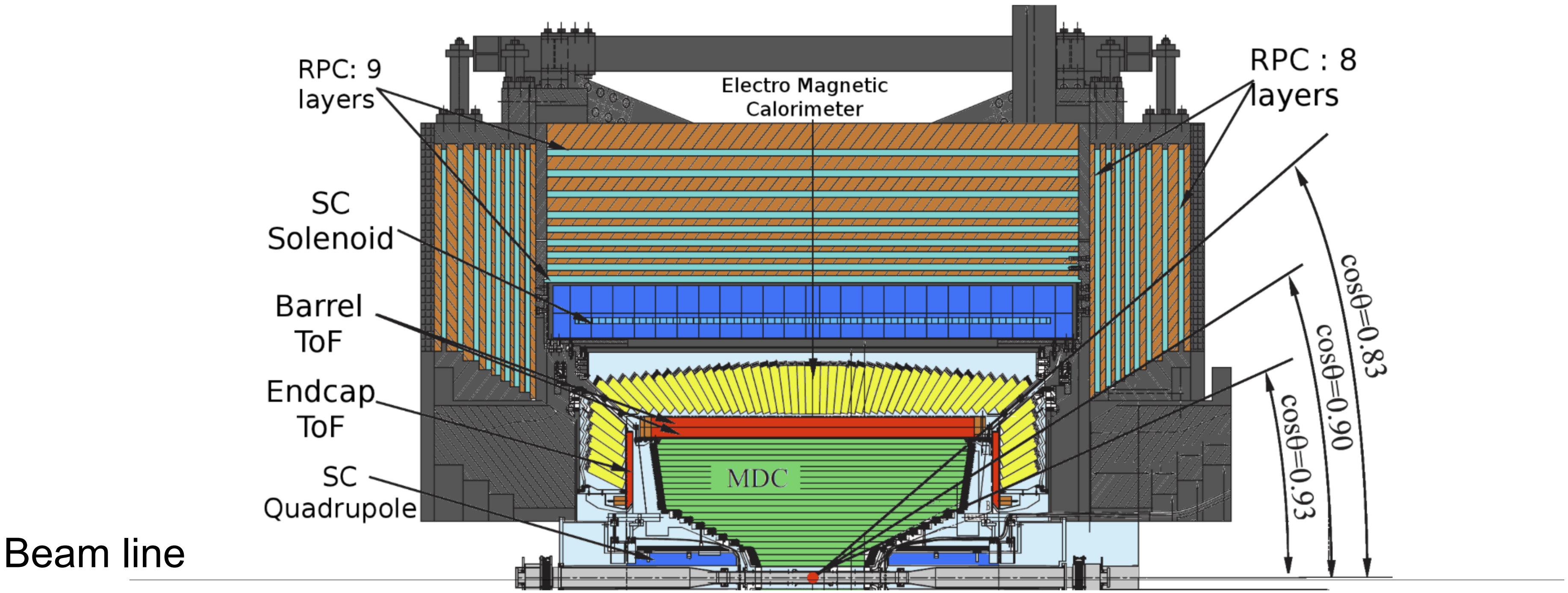

EMCalorimeter

CsI(Tl): $15X_0$,
λ_I = 171.5 g/cm^2, ρ = 4.53 g/cm^3
$P_{n,\bar{n}}$ = 52%

MUC

Iron + resistive plates
λ_I = 132.1 g/cm^2, ρ = 7.874 g/cm^3
56 cm Fe thickness in barrel
$P_{n,n}$ = ~96 %

TOF

2 Plastic scintillator layers BC408
Total width: 10 cm
Assuming p = 0.6 GeV/c
$\sigma(\bar{p}n)$= 1.5 $\cdot 10^2$ mb
$\sigma(pn)$= 0.4 $\cdot 10^2$ mb
N_H = 5.23 $\cdot 10^{22}$/cm3
N_C = 4.74 $\cdot 10^{22}$/cm3
$P_{\bar{n}}$ = 55%, P_n=13.5%

Analysis of $e^+e^- \rightarrow n\bar{n}$

Current analysis based only on **EMC information** and final state kinematics

Challenges:

Particle identification

- Only ~50% or n, $\bar{n}$ interact with EMC
- Energies of n, $\bar{n}$ not fully deposited in EMC
- Many secondary showers created → shower reconstruction very difficult
- Annihilation star makes it difficult to reconstruct back to back signature

Background

- large neutral backgrounds with photons ($\sigma(e^+e^- \rightarrow \gamma\gamma) >> \sigma(e^+e^- \rightarrow n\bar{n})$),$K_L$, ...
- huge background from beam associated processes

Trigger

- lower trigger efficiencies for purely neutral channels

Analysis of $e^+e^- \to n\bar{n}$

Analysis strategy:

- more than 1 shower in EMC and no charged tracks in MDC
- first identify $\bar{n}$:
  - highest energetic shower (0.5 GeV up to $E_{CM}/2 + m_n$)
  - energy deposited in 40° cone
  - number of hits in 40° cone
  - second moment of crystals in a shower
- then neutron identification:
  - shower energy (smaller than for $\bar{n}$)
  - most back to back shower to $\bar{n}$
- cuts against background
  - back to back signature between n and $\bar{n}$
  - no extra energy in EMC (not associated to n or $\bar{n}$)
  - reject low and large polar angles of n and $\bar{n}$

Background status

- Physics background negligible
- Beam background: studied with separated beam samples

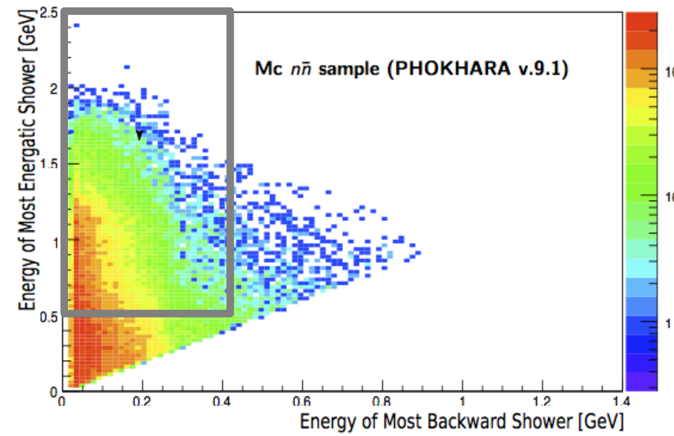

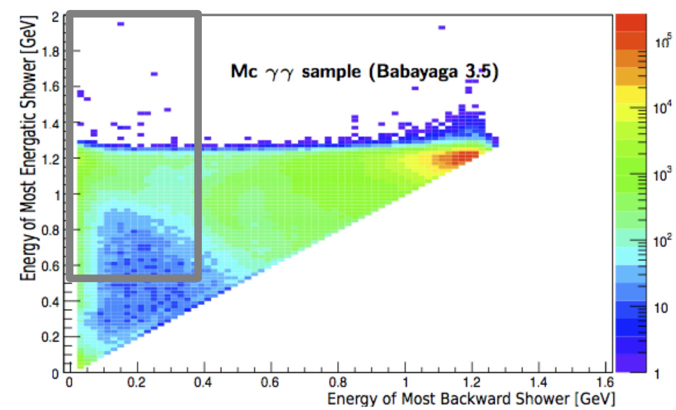

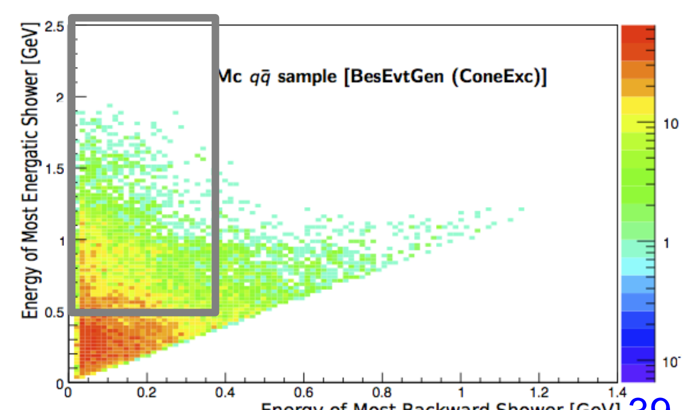

Analysis of $e^+e^- \rightarrow n\bar{n}$

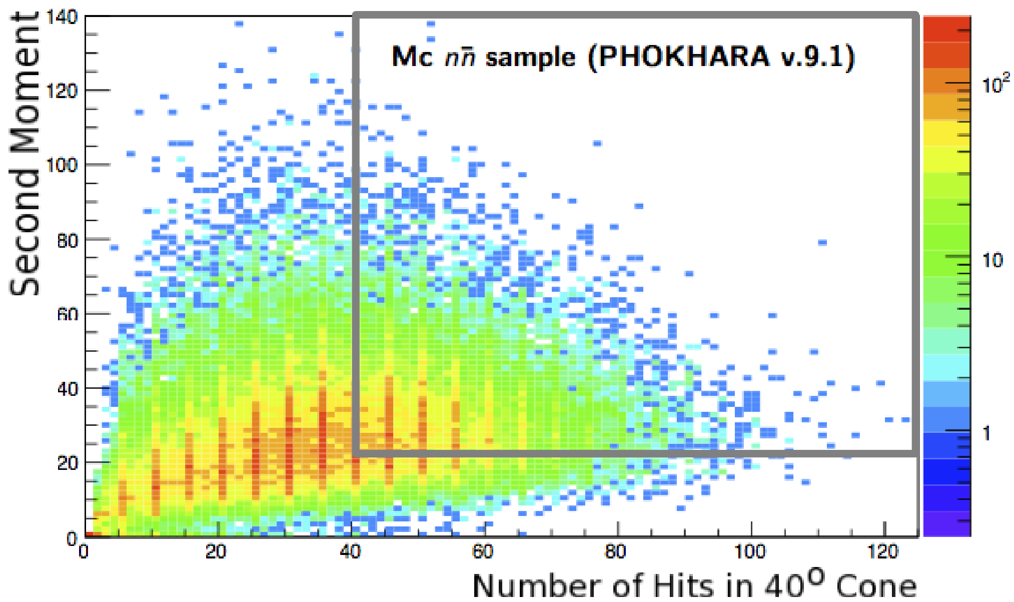

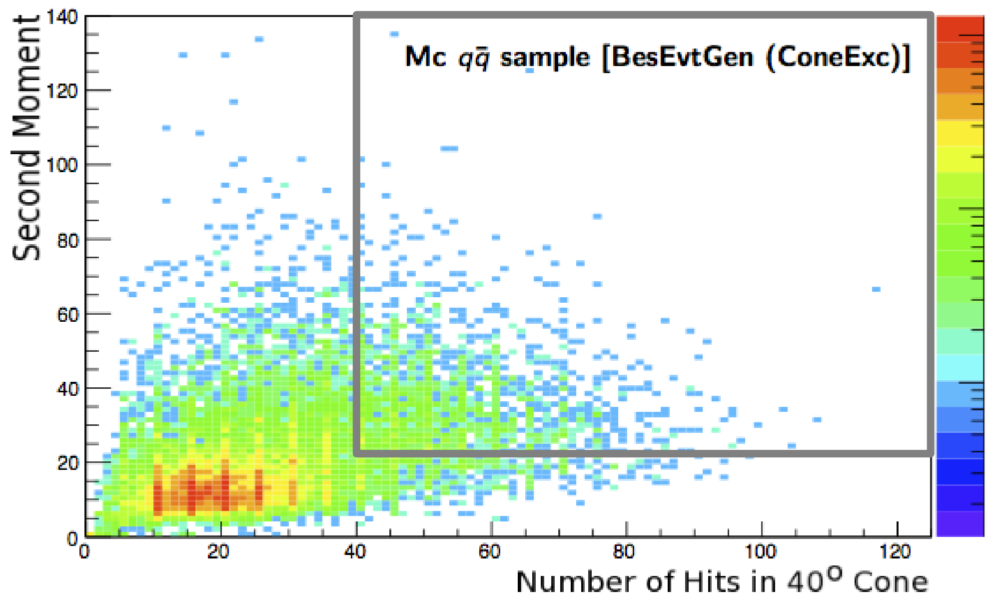

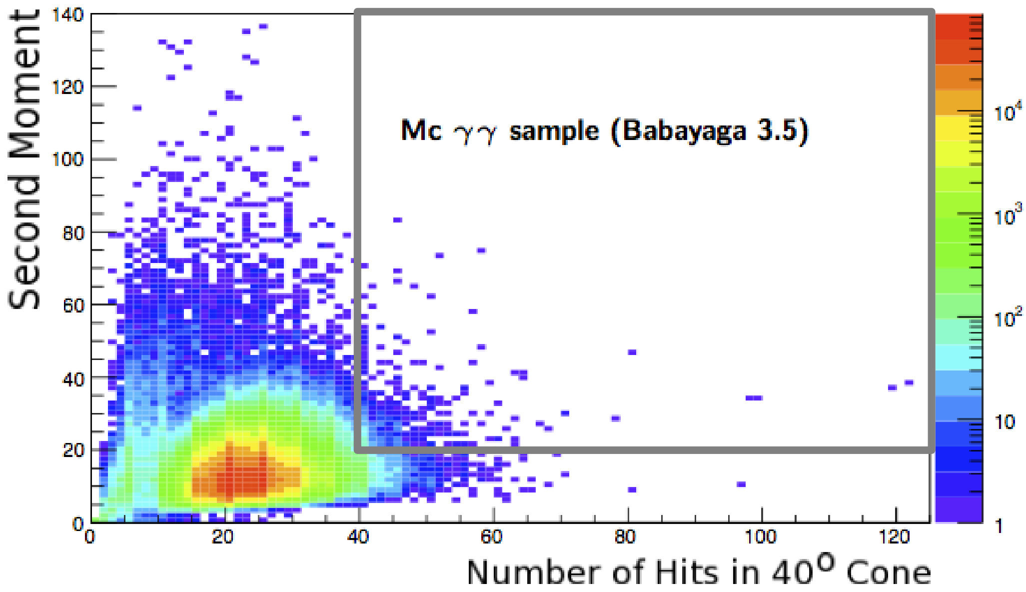

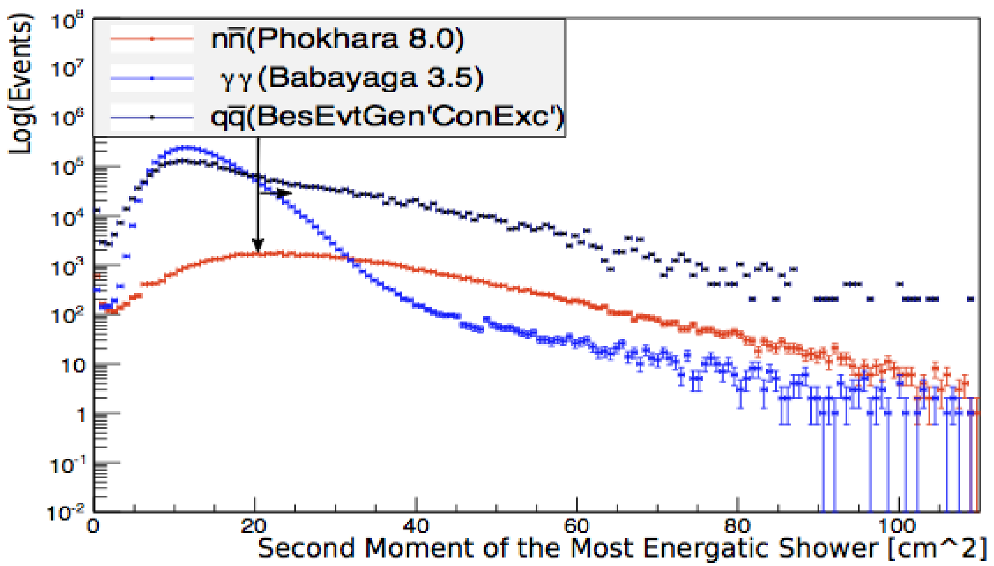

Prospects for $e^+e^- \to n\bar{n}$: $\sigma(n\bar{n})$, |G|, R...

$$\sigma^{\mathrm{Born}}(q) = \frac{N_{\mathrm{obs}(q)} - N_{\mathrm{bg}(q)}}{L \cdot \epsilon(q) R(q)}$$

$$|G(q^2)| = \sqrt{\frac{\sigma^{\mathrm{Born}}(q^2)}{(1 + \frac{2M^2}{q^2})(\frac{4\pi\alpha^2\beta C}{3q^2})}}$$

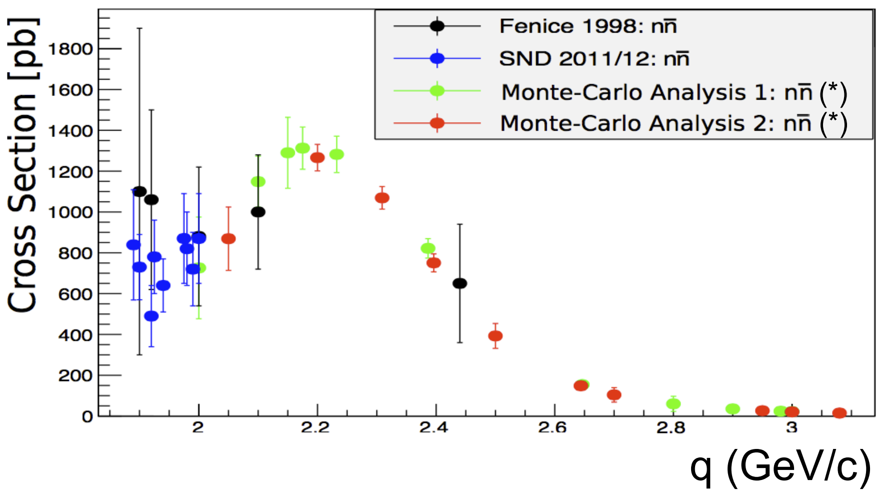

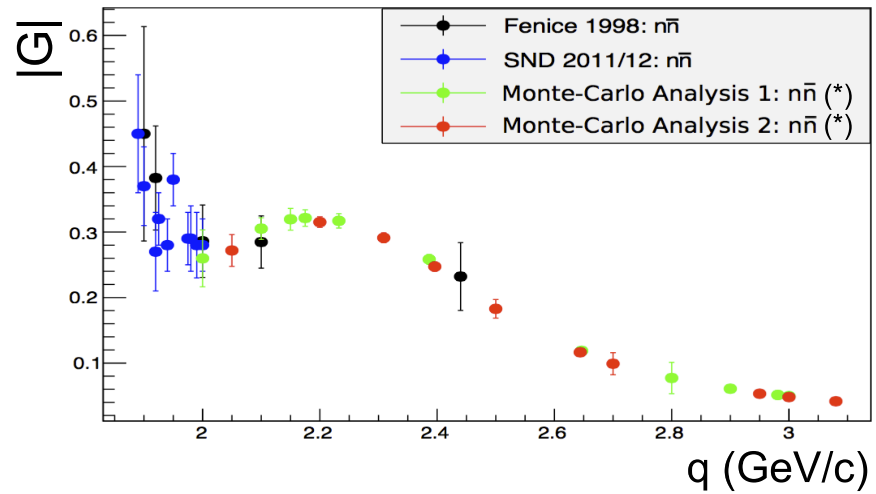

→ **Unprecedented statistics above 2.0 GeV**
Expected $\sigma(n\bar{n})$ accuracies between 6% (at 2.396 GeV) and 13% (at 3.0 GeV)

→ **First measurement of R and $|G_M|$ (and $|G_E|$) will be probably be possible at 2.396 GeV**

→ Current selection efficiencies (1% level) will be enhanced with the use of MUC and TOF detectors in the analysis

(*) Phokhara v9.1 [arXiv:1407.7995v2]. Default model based on SL and TL region measurements on neutron Ffs and $\sigma(n\bar{n})$

Summary

Summary & Outlook

- BESIII excellent laboratory for Nucleon form factor measurements: **energy scan + initial state radiation**

- First results on **Proton Form Factors** used a fraction of available scan data

- High statistics **energy scan between 2.0 and 3.08 GeV** will significantly improve Nucleon's FFs measurements

> **Protons: δR/R = 3 – 35%, δ|Gm|/|Gm| = 1 - 9%**
>
> → Perhaps sensitive to two-photon exchange?
>
> **Neutrons: δσ/σ = 6 – 13%, δ|G|/|G| = 3 – 7% or even better**
>
> → **First measurement of R** in the time-like region

Data from 2011 and 2012 will also be added

- Very exciting results from **ISR** on proton FFs expected very soon. Statistics similar to BaBar with only 7.4 fb^{-1}!

BESIII will keep on collecting high statistics at the main resonances → more statistics for ISR studies!

A new crystal zero degree detector will also enlarge ISR photon acceptance region

Backup

Analysis of $e^+e^- \to n\bar{n}\gamma_{ISR}$

Same challenges as for $e^+e^- \to n\bar{n}$ **and more!**

Detection of ISR photon needed for binning in q² $(q^2 = M_{n\bar{n}})$

↓

Only **tagged analysis in EMC** possible (no identification through 4-momentum conservation)

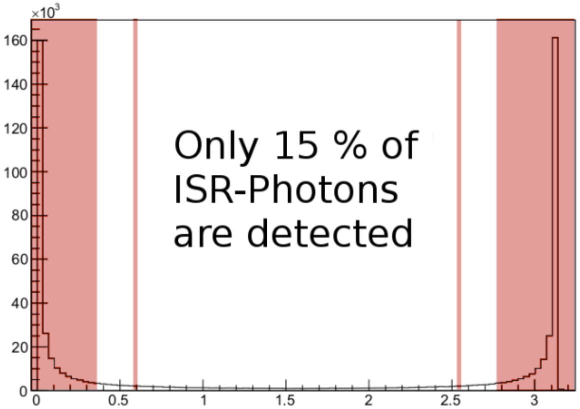

↓

Additional backgrounds:
$e^+e^- \to nn\pi^0(\eta)$, $e^+e^- \to \gamma\gamma(\gamma)$...

↓

Low efficiencies

Analysis of $e^+e^- \to n\bar{n}\gamma_{ISR}$

Analysis strategy:

- Energy deposition in EMC:

  EgammaISR has a sharp maximum

  $\bar{n}$ has large energy deposition

  n has small energy deposition

- Shape of e.m. Showers in EMC:

  Gamma ISR has narrow shower shape

  n and $\bar{n}$ have wider shower shapes

- Event kinematics:

  back to back signature between $n\bar{n}$-system and γ_{ISR} in e^+e^--CMS

  n and $\bar{n}$ back to back in $e^+e^-\gamma_{ISR}$-rest frame

Background status

Only $e^+e^- \to n\bar{n}\pi^0(\eta)$, $e^+e^- \to \gamma\gamma(\gamma)$ still present $\to$ Multi Variate Analysis with MC signal and bg validated with data

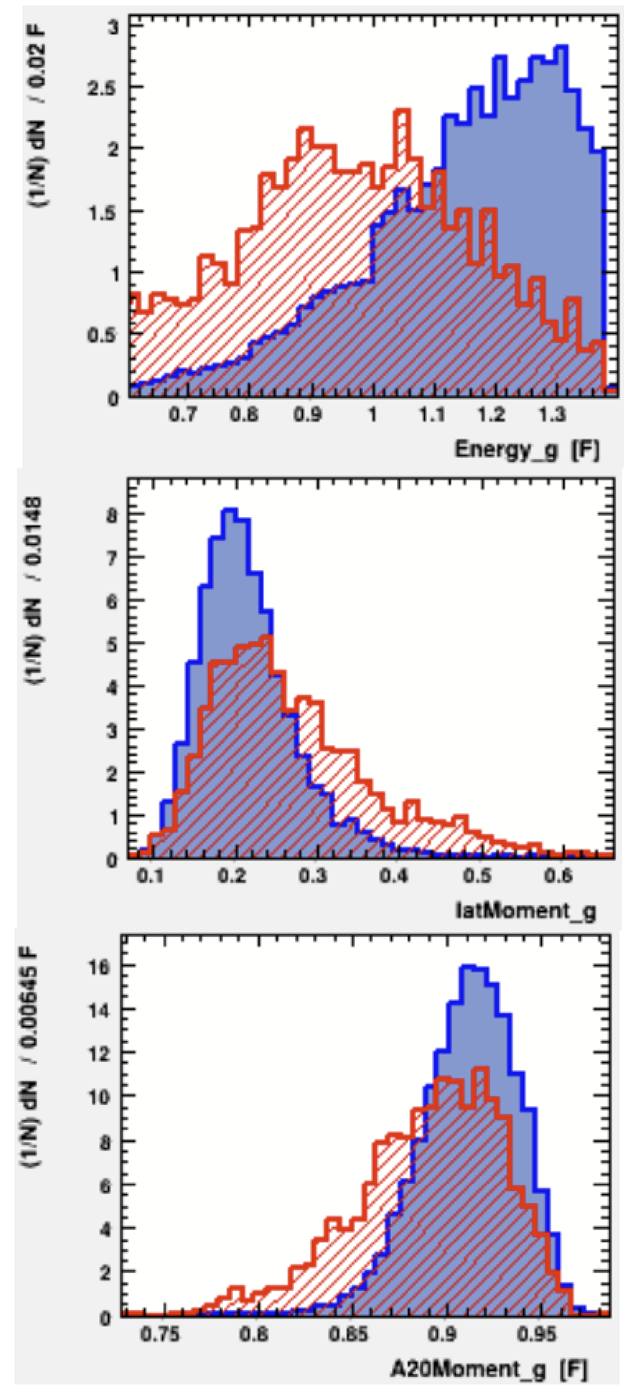

Analysis of $e^+e^- \to n\bar{n}\gamma_{ISR}$

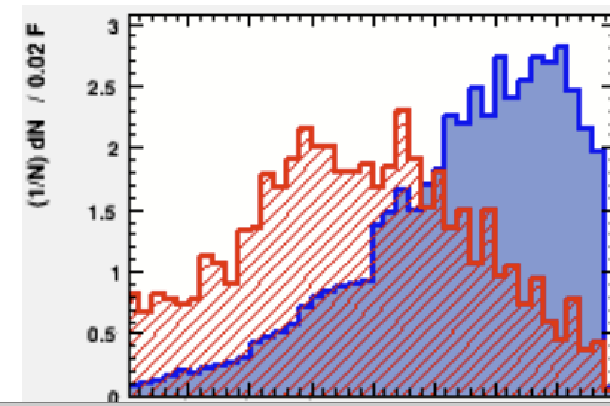

Analysis strategy:

- Energy deposition in EMC:

  EgammaISR has a sharp maximum

  $\bar{n}$ has large energy deposition

Problem: selection efficiencies at the 1‰ level !!

→ The use of TOF and MUC detectors in the analysis will definitely help!!

n and $\bar{n}$ back to back in $e^+e^-\gamma_{ISR}$-rest frame

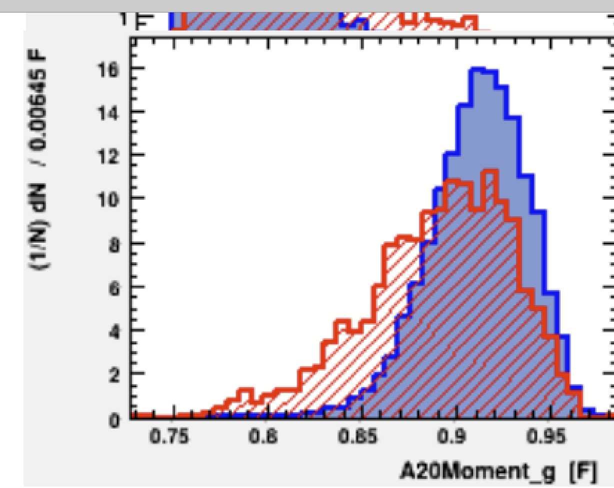

Background status

Only $e^+e^- \to n\bar{n}\pi^0(\eta)$, $e^+e^- \to \gamma\gamma(\gamma)$ still present → Multi Variate Analysis with MC signal and bg validated with data

BESIII data taking status & plan (run ~8 years)

	Previous data	BESIII present & future	Goal
J/ψ	BESII 58M	1.2 B 20* BESII	10 B
ψ'	CLEO： 28 M	0.5 B 20* CLEOc	3B
ψ''	CLEO： 0.8/fb	2.9/fb 3.5*CLEOc	20 /fb
Above open charm threshold	CLEO： 0.6/fb @ $\psi(4160)$	0.5/fb @ $\psi(4040)$ 2.3/fb@~4260, 0.5/fb@4360 0.5/fb@4600， 1/fb@4420	5-10 /fb
R scan & Tau	BESII	3.8-4.6 GeV at 105 energy points 2.0-3.1 GeV at 20 energy points	
Y(2175)		100 pb^{-1} (2015)	
$\psi(4170)$		3 fb^{-1} (2016)	

Peak luminosity achieved 9.98×10^{32} cm^{-2} s^{-1}

BESIII detector performance

Expt.	MDC Wire resolution	MDC dE/dx resolution	EMC Energy resolution
CLEO	110 μm	5%	2.2 – 2.4%
BABAR	125 μm	7%	2.67%
Belle	130 μm	5.6%	2.2%
BESIII	115 μm	$< 5\%$	2.3%

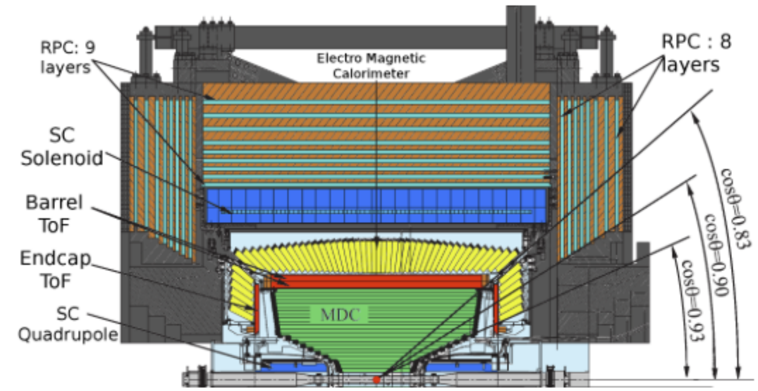

Expt.	TOF time resolution
CDF	100 ps
Belle	90 ps
BESIII	68 ps (Barrel) 100 ps (ETOF)

- 2015: Installation of new ETOF modules (MRPC, $\sigma_t \sim 60$ ps)
- Cylindrical GEM (CGEM) detector to replace inner part of MDC (Italy, IHEP, Germany, Sweden)
- Small-angle electron/photon tagger

ISR vs scan data: luminosity

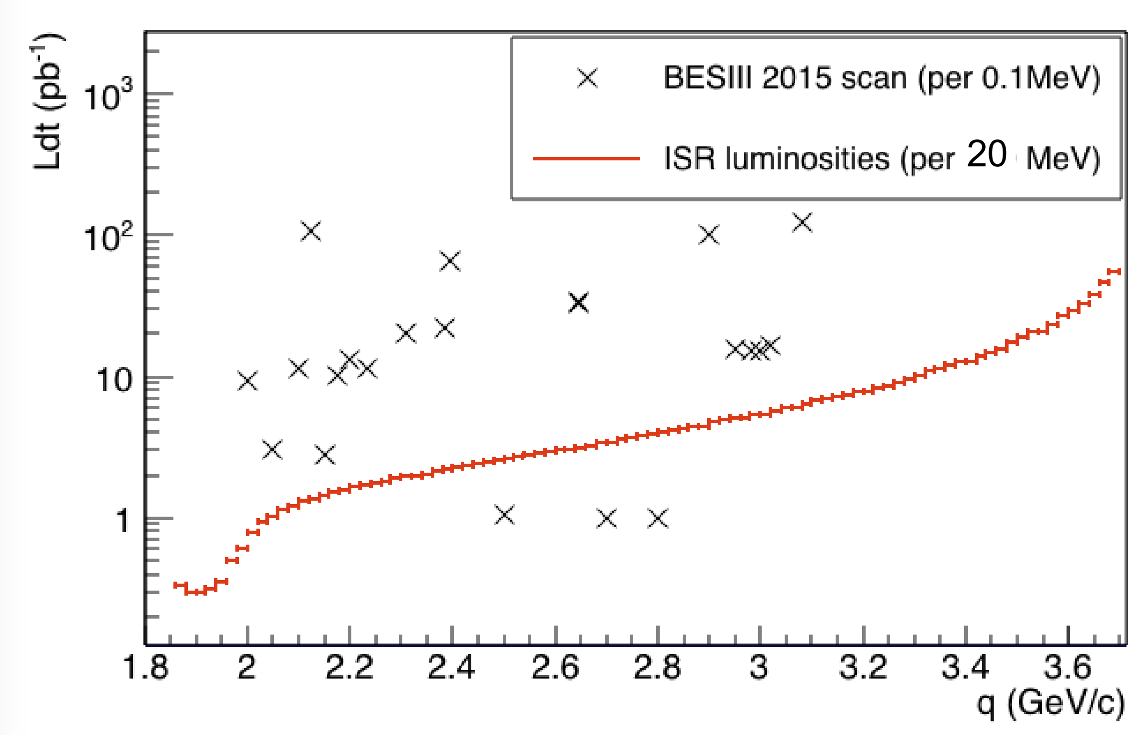

Data in TL region

[arXiv:1210.4689v1]

Direct production

$e^+e^- \to B\overline{B}$

Aqui falta SND

Exp.	Reaction	Year Publ.	Scan Points	Range [GeV]	$\mathcal{L}_{int}$ [pb^{-1}]	Events	Ref.
DM1	$e^+e^- \to p\bar{p}$	1979	4	1.925 – 2.180	0.4	~ 70	[14]
DM2	$e^+e^- \to p\bar{p}$	1983	6	1.975 – 2.25	0.5	~ 100	[15]
DM2	$e^+e^- \to p\bar{p}$	1990	1	2.4	0.2	7	[16]
DM2	$e^+e^- \to \Lambda\bar{\Lambda}$	1990	1	2.4	0.2	4	[16]
ADONE 73	$e^+e^- \to p\bar{p}$	1973	1	2.1	0.2	25	[11]
FENICE	$e^+e^- \to n\bar{n}$	1993	2	2.0 – 2.1	< 0.1	27	[19]
FENICE	$e^+e^- \to p\bar{p}$	1993	1	2.1	0.1	28	[19]
FENICE	$e^+e^- \to p\bar{p}$	1994	4	1.9 – 2.4	0.3	70	[12]
FENICE	$e^+e^- \to n\bar{n}$	1998	5	1.9 – 2.44	0.4	74	[13]
FENICE	$e^+e^- \to p\bar{p}$	1998	1	2.1	< 0.1	7	[13]
BES-II	$e^+e^- \to p\bar{p}$	2005	10	2.0 – 3.07	5	80	[17]
CLEO	$e^+e^- \to p\bar{p}$	2005	1	3.671	21	16	[18]
SND	$e^+e^- \to n\bar{n}$	2014	11	1.8-2.0	10	~5000	PRD90,112007(204)
BES3	$e^+e^- \to p\bar{p}$	2015	12	2.2324 – 3.671	157	~1370	PRD91,112004(2015)
CMD3	$e^+e^- \to p\bar{p}$	2015	12	1.885 –2.0023	6.8	~2700	Arxiv:1507.08013v2 (2015)

Annihilation

$p\bar{p} \to e^+e^-$

Exp.	Reaction	Year Publ.	Scan Points	Range [GeV]	Events	Ref.
M.S.T. Coll.	$p\bar{p} \to e^+e^-$	1976/77	2	near threshold	34	[22]
PS170	$p\bar{p} \to e^+e^-$	1991	4	near threshold	~ 2000	[23]
PS170	$p\bar{p} \to e^+e^-$	1991	4	1.94 – 2.05	~ 1300	[24]
PS170	$p\bar{p} \to e^+e^-$	1994	9	threshold – 2.05	~ 2000	[10]
E760	$p\bar{p} \to e^+e^-$	1993	3	3.0 – 3.6	29	[25]

ISR

$e^+e^- \to B\overline{B}\gamma$

Exp.	Reaction	Year Publ.	Mass Binning	Range [GeV]	$\mathcal{L}_{int}$ [pb^{-1}]	Events	Ref.
BaBar	$e^+e^- \to p\bar{p}$	2005	47	threshold – 4.5	$232 \cdot 10^3$	4025	[9]
BaBar	$e^+e^- \to \Lambda\bar{\Lambda}$	2007	12	threshold – 3.0	$232 \cdot 10^3$	138	[28]
BaBar	$e^+e^- \to \Lambda\bar{\Sigma}^0$	2007	4	threshold – 2.9	$232 \cdot 10^3$	24	[28]
BaBar	$e^+e^- \to \Sigma^0\bar{\Sigma}^0$	2007	5	threshold – 3.0	$232 \cdot 10^3$	18	[28]
BELLE	$e^+e^- \to \Lambda_c^+\Lambda_c^-$	2008	50	threshold – 5.4	$659 \cdot 10^3$	not cited	[29]
BaBar	$e^+e^- \to p\bar{p}$	2013	38	threshold – 4.5	$469 \cdot 10^3$	~6800	PRD87,092005(2013)
BaBar	$e^+e^- \to p\bar{p}$	2013	8	3.0 – 6.5	$469 \cdot 10^3$	~100	PRD88,072009(2013)

$e^+e^- \to p\bar{p}$ Phys. Rev. D91, 112004 (2015)

Extraction of $\sigma^{Born}(ee \to p\bar{p})$ for each scan point:

$$\sigma^{\text{Born}}(q) = \frac{N_{\text{obs}(q)} - N_{\text{bg}(q)}}{L \cdot \epsilon(q) R(q)}$$

- Efficiencies between 60% and 3% (ConExc)
- Radiative corrections up to LO in ISR (ConExc)
- Normalization to $e^+e^- \to e^+e^-$, $e^+e^- \to \gamma\gamma$ (Babayaga 3.5)

$\sqrt{s}$ (MeV)	N_{obs}	N_{bkg}	ε' (%)	L (pb^{-1})	σ_{Born} (pb)	$\lvert G\rvert$ ($\times 10^{-2}$)
2232.4	614 ± 25	1	66.00	2.63	$353.0 \pm 14.3 \pm 15.5$	$16.10 \pm 0.32 \pm 0.35$
2400.0	297 ± 17	1	65.79	3.42	$132.7 \pm 7.7 \pm 8.1$	$10.07 \pm 0.29 \pm 0.31$
2800.0	53 ± 7	1	65.08	3.75	$21.3 \pm 3.0 \pm 2.8$	$4.45 \pm 0.31 \pm 0.29$
3050.0	91 ± 10	2	59.11	14.90	$10.1 \pm 1.1 \pm 0.6$	$3.29 \pm 0.17 \pm 0.09$
3060.0	78 ± 9	2	59.21	15.06	$8.5 \pm 1.0 \pm 0.6$	$3.03 \pm 0.17 \pm 0.10$
3080.0	162 ± 13	1	58.97	30.73	$8.9 \pm 0.7 \pm 0.5$	$3.11 \pm 0.12 \pm 0.08$
3400.0	2 ± 1	0	63.34	1.73	$1.8 \pm 1.3 \pm 0.4$	$1.54 \pm 0.55 \pm 0.18$
3500.0	5 ± 2	0	63.70	3.61	$2.2 \pm 1.0 \pm 0.6$	$1.73 \pm 0.39 \pm 0.22$
3550.7	24 ± 5	1	62.23	18.15	$2.0 \pm 0.4 \pm 0.6$	$1.67 \pm 0.17 \pm 0.23$
3600.2	14 ± 4	1	62.24	9.55	$2.2 \pm 0.6 \pm 0.9$	$1.78 \pm 0.25 \pm 0.35$
3650.0	36 ± 6	4	61.20	48.82	$1.1 \pm 0.2 \pm 0.1$	$1.26 \pm 0.11 \pm 0.07$
3671.0	6 ± 2	0	51.17	4.59	$2.2 \pm 0.9 \pm 0.8$	$1.84 \pm 0.37 \pm 0.33$

Gain From Raw Data Analysis

- From raw data: TOF and MUC information for neutrals

M. Ablikim et al. / Nuclear Instruments and Methods in Physics Research A 614 (2010) 345–399

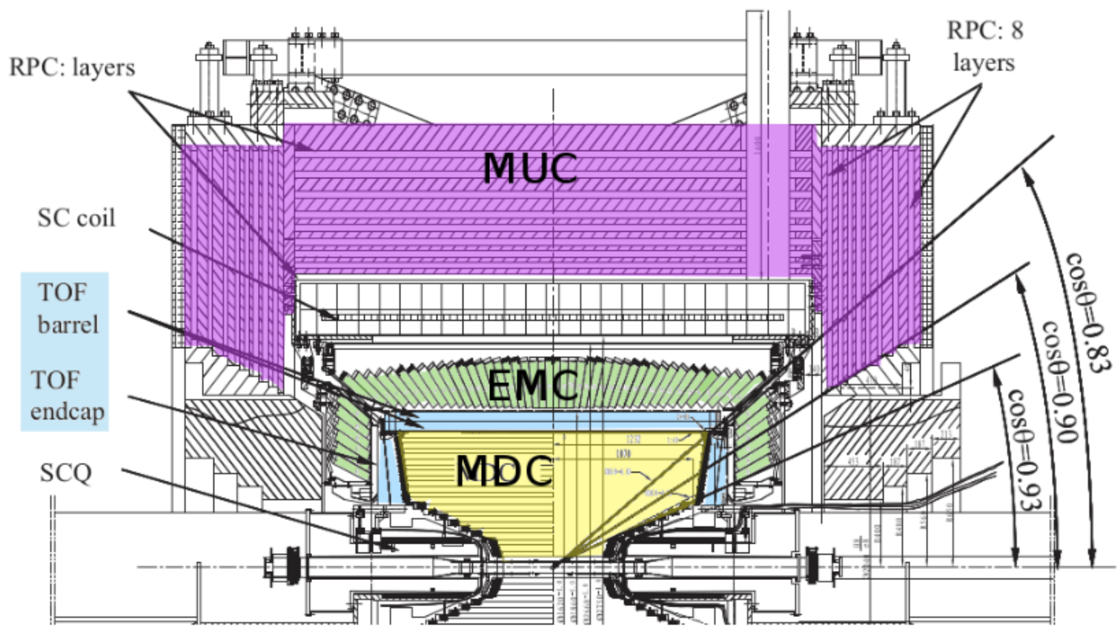

(a) BESIII detector

- What do we hope to achieve with these two subdetectors?
  - → More statistics: drop tagging the neutron, tag only $\overline{n}$ (and γ_{ISR})
  - → Suppress bg: γ's are faster than $\overline{n}$ and don't reach MUC

Detect Cosmic Rays With MUC

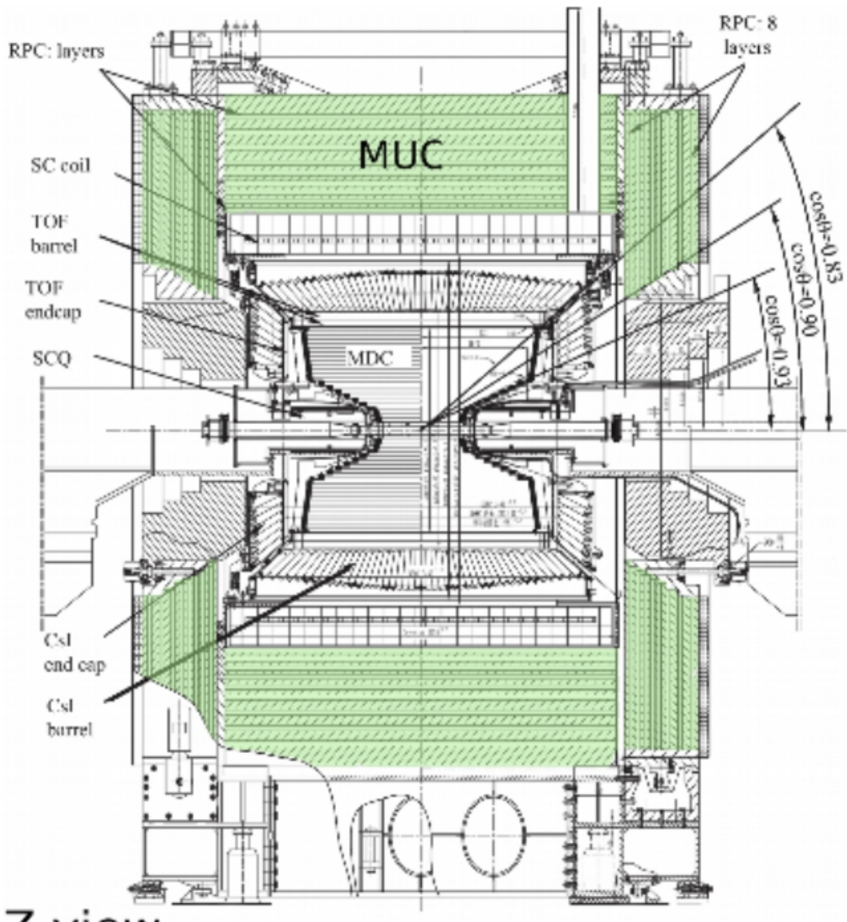

Fig. 1. Schematic drawing of the BESIII detector.

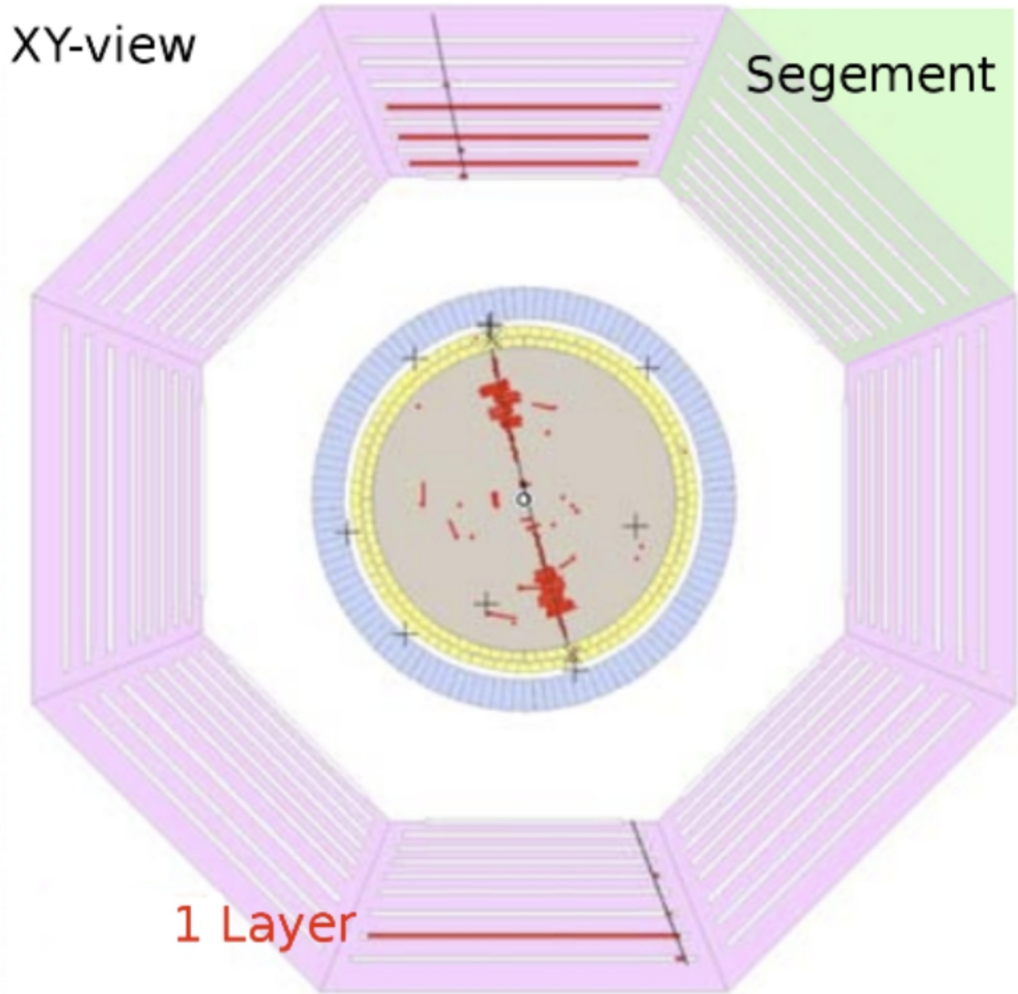

Fig. 1. The illustration of one cosmic ray goes through the BESIII detecter.

One Method To Use MUC As $\overline{n}$ Detector

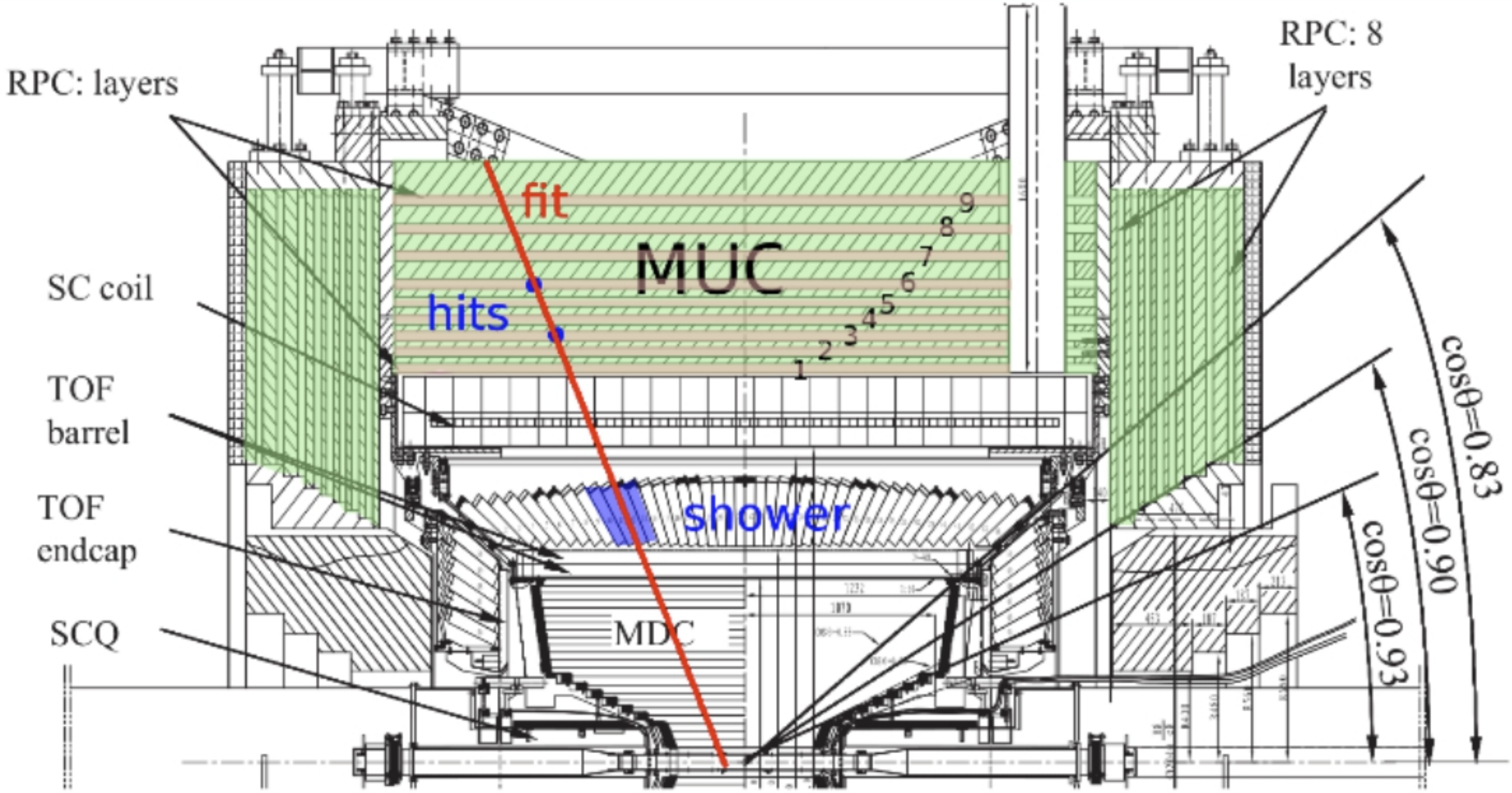

- Not possible for hits in 2 even layers (only MuC Φ-position)
- For hits in 2 odd layers (only MuC z-position) we have at least the Φ-position of segment → need to be studied!

- But if we detect MUC hits in odd **and** even layer:
  → Linear fit through MUC signal, EMC shower and Vertex
  → If no signal from n, this should be enough to select signal

Proposal: The Crystal Zero Degree Detector

An Alternative

crystals (option: $PbWO_4$)

flash ADC

realtime event correlation

$PbWO_4$

density	$8.28\,g/cm^3$
radiation length	$0.89\,cm$
Moliere radius	$2.00\,cm$
τ_1 (fast component, 97 %)	$6.5\,ns$
τ_2 (slow component, 3 %)	$30.4\,ns$
relative lightyield	0.6 % at $20^\circ C$
compared to NaI	2.5 % at $-25^\circ C$

Spatial considerations

- ISR peaked at $\theta = 0°$ and $180°$ $\Rightarrow$ position of detector
- Limited space $\Rightarrow$ compact design
- Bremsstrahlung even stronger peaked towards $\theta = 0°$ and $180°$ $\Rightarrow$ small gap

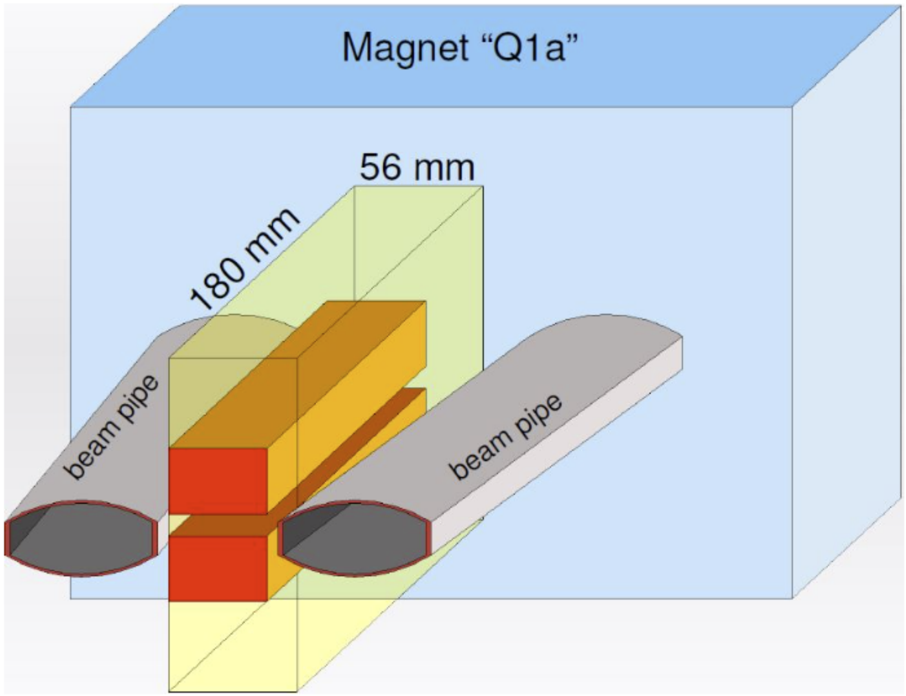

Geometry

- Similar layout as ZDD (2 blocks divided by a 1 *cm* gap)
- 3×4 crystals per block
- $1 \times 1 \times 14\,cm^3$ crystals

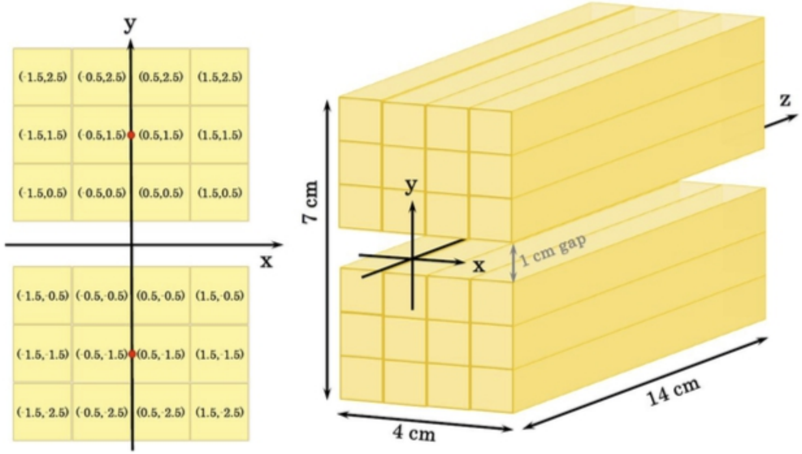

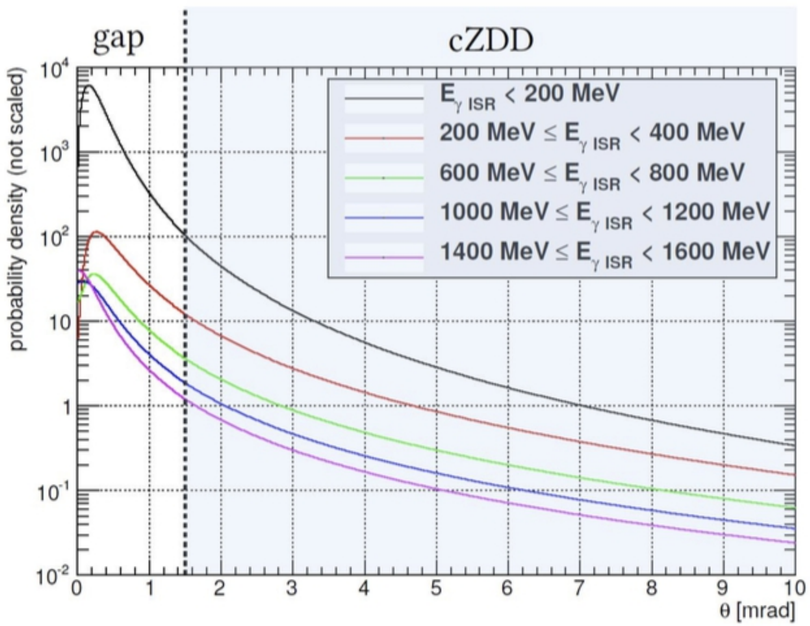

- Maximum of ISR distribution out of acceptance
- Note: log-scale!
- But: reduction of bremsstrahlung

Pion FF in BESIII

$e^+e^- \to \pi^+\pi^-\gamma_{ISR}$ arXiv:1507.08188 (submitted to PLB)

- Goal: **hadronic vacuum polarization contribution to $a_\mu = \frac{(g_\mu-2)}{2}$**

$$a_\mu^{SM} = a_\mu^{QED} + a_\mu^{weak} + a_\mu^{hadr}$$

→ most relevant contribution to a_μ^{hadr} below 1 GeV: $\sigma(e^+e^- \to \pi^+\pi^-)$

$$|F_\pi|^2(q^2) = \frac{3q^2}{\pi\alpha^2\beta^3}\sigma^{dressed}_{\pi^+\pi^-}(q^2)$$

Disagreement between existing measurements limits knowledge of a_μ

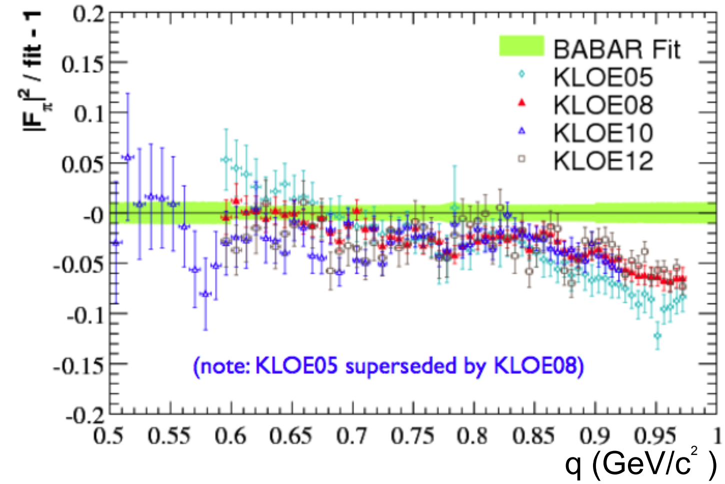

- Features of BESIII analysis:
  - 2.9 fb-1 from Ψ(3770)
  - studied range between 600 – 900 MeV
  - only tagged analysis possible below 1 GeV
  - main background from $e^+e^- \to \mu^+\mu^-\gamma_{ISR}$ prefectly understood (<1‰)
  - luminosity from BhaBha events → 0.5% accuracy (Babayaga NLO)
  - FF fit function: Gounaris-Sakurai parametrization
  - radiative corrections from Phokhara v8.0

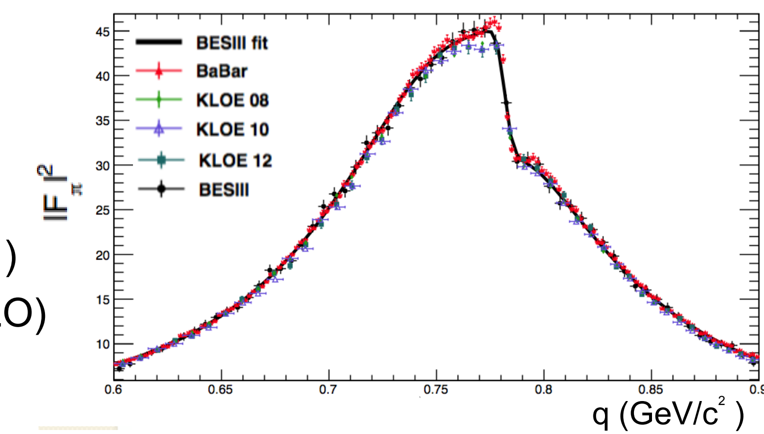

Syst. uncertainty in cross section 0.9%

Compatible with prev. measurements (1σ)

More than 3σ deviation wrt $(g_\mu-2)^{SM}$ prediction confirmed

Data from untagged analysis and above Ψ(3770) will be used

Analysis will be extended below 600 MeV and above 900 MeV

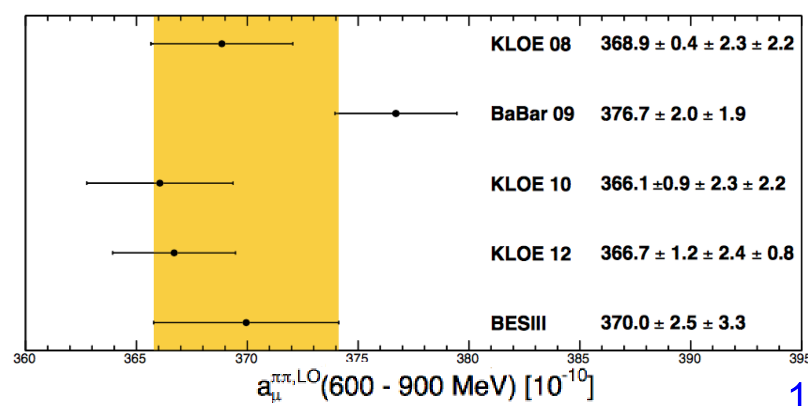

Hyperon EM FFs in BESIII

$e^+e^- \to \Lambda\bar{\Lambda}$ (BESIII Preliminary!!)

Based on 40.5 pb^{-1} collected in 4 scan points between 2.2324 – 3.08 GeV in 2012

- at E_{CM} = 2.2324 GeV (**1 MeV from threshold!!**)

  From $\Lambda \to p\pi^-$ and $\bar{\Lambda} \to \bar{p}\pi^+$ ($BR_{p\pi}$ = 64%)
  - well defined $p_{\pi+}$ and $p_{\pi-}$ and possible $\bar{p}$-annihilation

  From $\bar{\Lambda} \to \bar{n}\pi^0$ ($BR_{n\pi 0}$ = 36%)
  - $\bar{n}$-annihilation and well defined $p_{\pi 0}$

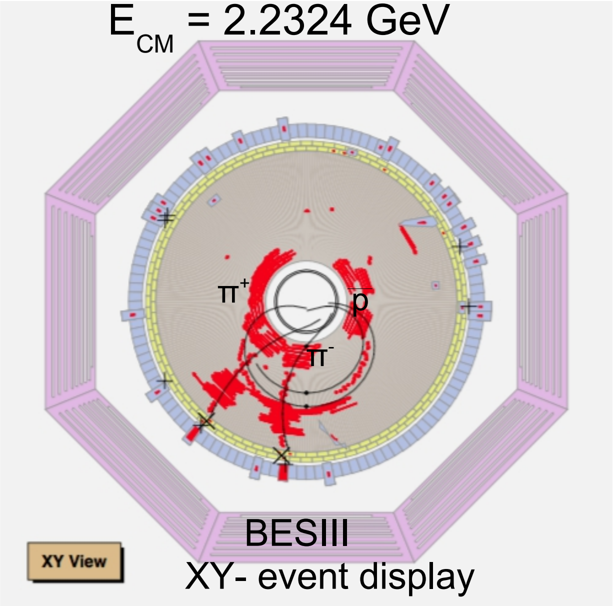

- at E_{CM} ≥ 2.4 GeV, from $\Lambda \to p\pi^-$ and $\bar{\Lambda} \to \bar{p}\pi^+$
  - p, $\bar{p}$, π^- and π^+ from interaction vertex, in time, $\Lambda\bar{\Lambda}$ back to back, $E_{\Lambda,\bar{\Lambda}} = E_{CM}/2$ ...

Results:

$\sqrt{s}$ (GeV)	Channel	σ^{Born}(pb)	$\lvert G\rvert$ ($\times 10^{-2}$)
2.2324	$\Lambda \to p\pi^-, \bar{\Lambda} \to \bar{p}\pi^+$	$325 \pm 53 \pm 46$	
	$\bar{\Lambda} \to \bar{n}\pi^0$	$300 \pm 100 \pm 40$	
	combined	$318 \pm 47 \pm 37$	$63.2 \pm 4.7 \pm 3.7$
2.4000	$\Lambda \to p\pi^-, \bar{\Lambda} \to \bar{p}\pi^+$	$133 \pm 20 \pm 19$	$12.9 \pm 1.0 \pm 0.9$
2.8000		$15.3 \pm 5.4 \pm 2.0$	$4.2 \pm 0.7 \pm 0.3$
3.0800		$3.9 \pm 1.1 \pm 0.5$	$2.21 \pm 0.31 \pm 0.14$

$e^+e^- \to \Lambda\bar{\Lambda}$ (BESIII Preliminary!!)

No Coulomb term for neutral baryon pairs → cross section should vanish at threshold

$$\sigma^{Born}(q^2) = \frac{4\pi\alpha^2\beta}{3q^2}\left[|G_M(q^2)|^2 + \frac{2M^2}{q^2}|G_E(q^2)|^2\right]$$

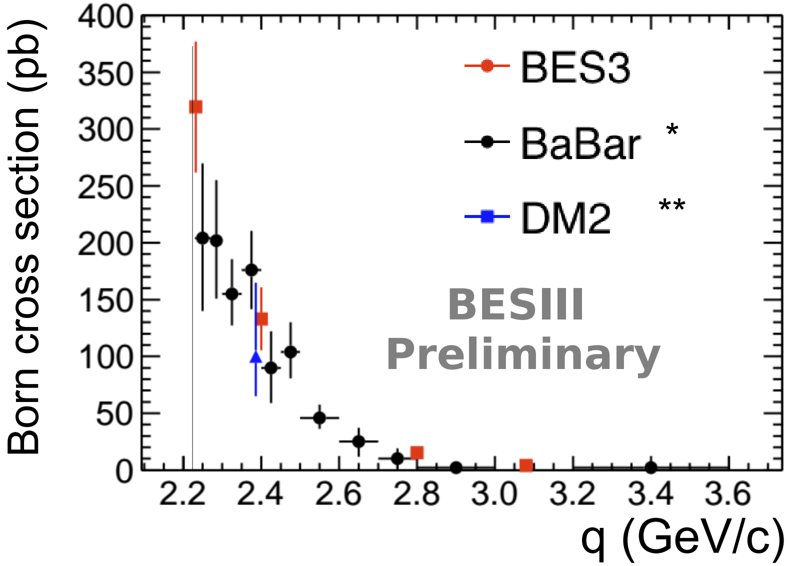

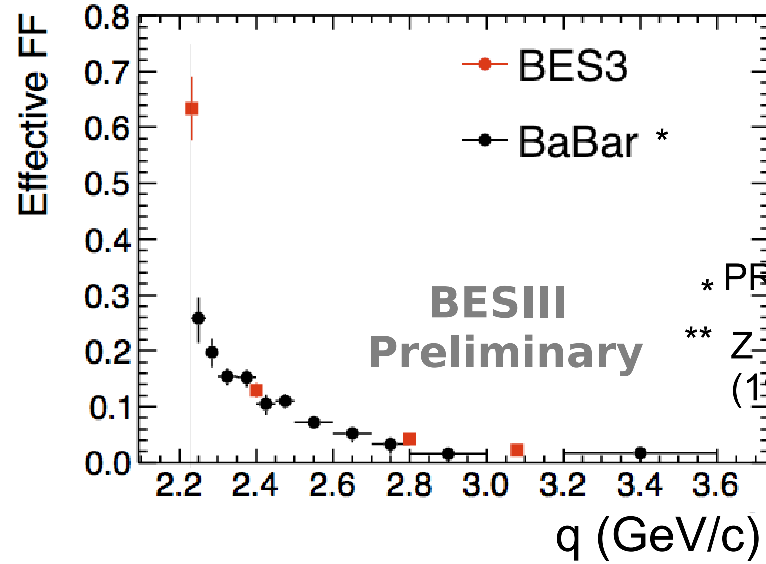

* PRD76,092006 (2007)

** Z Phys C48, 23 (1990)

Precision increased by at least 10% for low q^2 and even more above 2.4 GeV

→ Origin of unexpected behavior? Coulomb interaction at quark level?(***)

→ Precison measurement forseen by BESIII with 2015 data

*** Eur. Phys. J. A39:315-321(2009)

Prospects for $e^+e^- \rightarrow$ Hyperons

From 2015 scan full determination of lambda- FFs possible:

- Imaginary part of FFs leads to polarization observables:

  Parity violating decay: $\Lambda \rightarrow p\pi$

$$\frac{dN}{d\cos\theta_p} \propto 1+\alpha_\Lambda P_n \cos\theta_p \quad \text{and} \quad P_n = -\frac{\sin 2\theta \sin\Delta\phi/\tau}{R\sin^2\theta/\tau+(1+\cos^2\theta)/R} = \frac{3}{\alpha_\Lambda}\langle\cos\theta_p\rangle$$

Θ_p : Angle between proton and polarization axis in Λ-CM

Θ_Λ: Λ polar angle in CM

Φ : relative phase between G_E and G_M

Expected statistical accuracies for P_n between 6 and 17%

Expected statistical accuracies for $R_{em} = |G_E|/|G_M| = 1$ between 14 and 29%

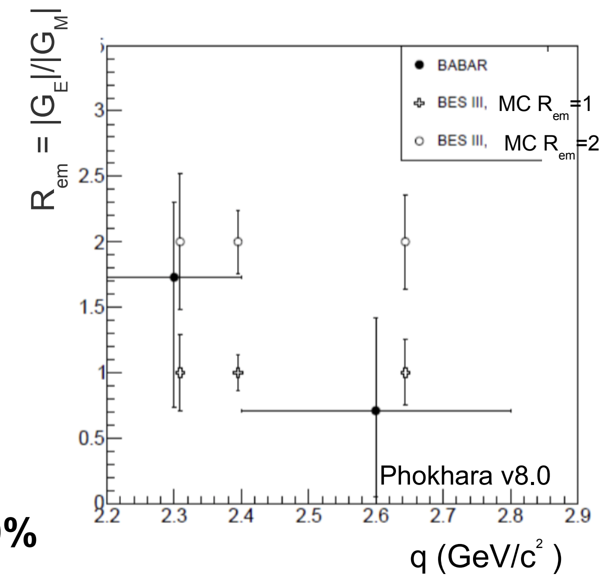

- Also available from threshold (2015, 2014, 2011 data):

  $ee \rightarrow \Lambda\bar{\Sigma}^0, \Sigma^0\bar{\Sigma}^0, \Sigma^-\bar{\Sigma}^+, \Sigma^+\bar{\Sigma}^-, \Xi^0\bar{\Xi}^0, \Xi^+\bar{\Xi}^-, \Omega^+\bar{\Omega}^-, \Lambda_c^-\bar{\Lambda}_c^+$

measurements of effective FF and R_{em} and P_n at single energy points possible

$ee \rightarrow \Lambda\Sigma^0, \Sigma^0\Sigma^0$ previously measured by BaBar, no R_{em} extraction possible

measurements of effective FF, R_{em} and $|G_M|$ at threshold possible